Soft Robots Modeling: A Structured Overview

Costanza Armanini ⓘ, *Member, IEEE*, Frédéric Boyer, Anup Teejo Mathew ⓘ,
Christian Duriez ⓘ, *Senior Member, IEEE*, and Federico Renda ⓘ, *Member, IEEE*

Abstract—The robotics community has seen an exponential growth in the level of complexity of the theoretical tools presented for the modeling of soft robotics devices. Different solutions have been presented to overcome the difficulties related to the modeling of soft robots, often leveraging on other scientific disciplines, such as continuum mechanics, computational mechanics, and computer graphics. These theoretical and computational foundations are often taken for granted and this leads to an intricate literature that, consequently, has rarely been the subject of a complete review. For the first time, we present here a structured overview of all the approaches proposed so far to model soft robots. The chosen classification, which is based on their theoretical and numerical grounds, allows us to provide a critical analysis about their uses and applicability. This will enable robotics researchers to learn the basics of these modeling techniques and their associated numerical methods, but also to have a critical perspective on their uses.

Index Terms—Dynamics, flexible robots, kinematics, modeling, control, and learning for soft robots.
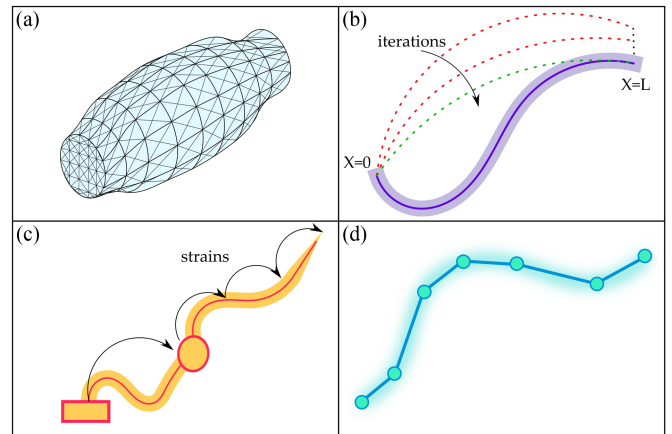
Fig. 1. Some resolution methods that have been distinguished in this review. (a) FEM, (see Section IV-A). (b) Shooting method (see Section V-A2). (c) Relative modal-Ritz reduction (Section V-B4). (d) Pseudorigid approach (see Section VII-B).

I. INTRODUCTION

THE term *soft robot* appeared for the first time in a scientific paper in [1], describing a McKibben pneumatic artificial muscle a family of braided pneumatic actuators developed in the 50 s to assist polio patients. Even though they were not explicitly called *soft robots*, McKibben actuators represent the first example of a robotic device exploiting its compliance to achieve improved performances with respect to their exclusively rigid counterpart. Since then, soft robotics has been one of the fastest growing research community in the last decades. Many different soft robotics devices and actuators have been presented, ranging

in almost every possible technological field, from biomedical engineering to aerospace and underwater robotics. The increasing interest in soft robotics is demonstrated by the vast number of review papers that have been published to summarize the employed techniques, the achievements and the future prospects of this research field [2], [3], [4], [5]. Among the available reviews on the theoretical modeling components, some have been published for specific groups of approaches [6], [7], [8], [9], [10], some for specific application fields [11], [12], and others for specific families of robots [13].

Unlike traditional rigid robots, soft robots are infinite-dimensional systems whose time evolution is governed by highly nonlinear partial differential equations (PDEs), generally not analytically integrable. Based on this observation, the search for a tradeoff between accuracy and numerical usability for robotic purposes (such as control and optimization), is undoubtedly the great challenge of soft robot modeling. For the first time, we present here a comprehensive literature review of the techniques that have been presented to model soft and continuous robots. Given the enormous quantity and diversity of contributions on this theme in recent years, choices had to be made to classify them. The chosen classification is based on the mathematical techniques themselves (see Fig. 1), and not on their uses (design, simulation, control). Although this choice may seem a bit arbitrary at first sight, it has the great advantage of highlighting the structural similarities and differences that gather and/or discriminate all the modeling approaches proposed so far in the field. Moreover, it allows us to go back to the theoretical

Costanza Armanini, Anup Teejo Mathew, and Federico Renda are with the Department of Mechanical Engineering, Khalifa University of Science and Technology, Abu Dhabi 127788, UAE, and also with the Khalifa University Center for Autonomous Robotic Systems, Khalifa University of Science and Technology, Abu Dhabi 127788, UAE (e-mail: costanza.armanini@ku.ac.ae; anup.mathew@ku.ac.ae; federico.renda@ku.ac.ae).

Frédéric Boyer is with the LS2N Laboratory, Institut Mines Telecom Atlantique, 44307 Nantes, France (e-mail: frederic.boyer@imt-atlantique.fr).

Christian Duriez is with the Inria, CNRS, Centrale Lille, Team DEFROST, University Lille, 59000 Lille, France (e-mail: christian.duriez@inria.fr).

roots of the different approaches and to give their historical origins, sometimes from other communities. We believe that this will enable robotics researchers to learn the basics of these modeling techniques and their associated numerical methods, and to have a critical perspective on their uses. The rest of this article is organized as follows. In Section II, some general concepts are drawn and the classification employed to discuss all the modeling approaches is presented. In Section III, we present the formulation of models that are based on continuum mechanics theories, while their numerical resolution is presented in Sections IV and V. In Section VI, we present the approaches, which rely on the hypothesis that the deformed shape of the robot follows a specific geometrical curve. Proceeding with the level of discretization, in Section VII, the approaches that arise from an a priori discretization of the soft body are presented, while in Section VIII, data-driven models are discussed. Section IX presents the software implementation of the proposed approaches. Finally, Section X concludes this article.

II. BASIC CONCEPTS AND CLASSIFICATION

Mechanical modeling is a set of mathematical techniques, allowing us to represent the evolution of a material system. It is defined by the following key concepts [14], [15].

1) *Configuration:* The set of position of the system's particles compatible with the internal (joints) and the external [geometric boundary conditions (BCs)] kinematic constraints. At any given time, the configuration of a mechanical system defines a subset of the ambient Euclidean space.
2) *Generalized coordinates:* A set of parameters describing any configuration. They are the coordinates of a unique point in an abstract space or "configuration space." They can be *absolute* when they refer to a fixed inertial frame, or *relative* when they refer to a moving frame covarying together with the system.
3) *Kinematic map:* It takes as input the generalized coordinates and it returns the configuration of the system. This is also called *forward kinematics*, while the *inverse kinematics* represents exactly the opposite process, i.e., the calculation of the coordinates (typically, the actuation ones) required to obtain a specific configuration of the system.
4) *Dynamic principle:* Such as Newton's laws, d'Alembert's principle, or Hamilton's principle. Such a principle provides the equations of motion (EoM) of the system governing the temporal evolution of its configurations.

The abovementioned characteristics of a mechanical model can be identified relatively easily for a traditional rigid robot. However, this is not the case for soft robots, due to their continuum nature. In fact, while traditional rigid robots can be fully represented by some finite discrete set of frames, in soft robotics the robot is a continuum of particles. Let us draw some general considerations on the main steps that are required to obtain a model for a continuum body. In the Lagrangian description of solid continuum mechanics, the body's *configuration* is parameterized through *positional* fields, which depend both on time and on the material coordinates, i.e., a set of continuous labels

X that identifies each particle. In particular, X can be defined as the coordinates of the particles of the body when it is in a stress-less configuration, called *reference configuration*. The motion of a continuum body is defined by a continuous sequence of configurations along time. A change in the configuration of a continuum body results in a *displacement*, which usually has two components: a rigid-body displacement and a *deformation*. To describe the internal deformation state of the body, it is necessary to define its strain (time) rate, which is a combination of the gradient of the velocity fields. The definition of the strains needs to be objective, i.e., observer independent. Finally, beyond kinematics, the closed formulation describing the time evolution of a continuum medium is given by the following.

1) a principle of the dynamics (as before), providing the PDEs relating the stress with the acceleration of the particles and the external forces applied inside and across the boundaries of the medium;
2) a set of geometric BCs;
3) a constitutive law that relates the time evolution of the stress to that of the strains.

The resulting dynamic equations are, in general, highly non-linear and characterized by an infinite-dimensional configuration space. The soft robotics modeling literature could be viewed as the story of how these extremely complex equations, when applied to soft robots, can be discretized and solved. It should be noted that *discretization* and *reduction* are two distinct concepts that should not be confused. A *discretization* is employed to obtain a numerical solution to the nonlinear problem and, for example, the finite differences methods fall in this category. On the other side, a *reduction* consists in the depiction of a basis of functions allowing a proper description of the kinematic fields of the body. These features are not always clearly expressed in the developing of a theoretical model, or they might be implicitly imposed by the assumptions of the model itself or its numerical resolution. One of the aims of this work is to shed light on the underline structure of the proposed models using a unified language, which facilitate their understanding and comparison. With this as a guideline, we classified the modeling of soft robots as follows.

1) *Continuum mechanics models:* They are characterized by a continuous (infinite-dimensional) configuration space, and on physical considerations about the soft bodies deformations. As such, they benefit from a physically rigorous definition of the kinetic and potential energy of the system. This family of models can employ both absolute and relative coordinates reduction and they are derived from continuum mechanics theories. When no specific assumptions are made, they are based on the classical three-dimensional continuum mechanics theory, while other approaches have been presented for surface structures (shells, membranes) or slender structures (beam, rods). In particular, the latter include Cosserat, Kirchhoff, and nonlinear Euler Bernoulli beam theories, which are frequently employed in soft robotics.

2) *Geometrical models:* They are based on geometrical assumptions on the deformed shape undertaken by the soft body when specific loads are applied. For this group, the central role is taken by the generalized coordinates, on which the system's kinetic and potential energy are defined. In particular, two main

groups emerged. The first one includes the "functional" models, which all rely on the assumption that the deformed shape of the body resembles a theoretical space curve represented by a specific mathematical function. In this case, the generalized coordinates are usually absolute in nature. The second group includes the widely known piecewise-constant-curvature (PCC) models, which are based on the discretization of the continuous soft body in a finite number of sections having circular arc shape, with intrinsically relative coordinates.

3) *Discrete material models:* As the name suggests, these models are based on a discretization of the continuous body in a finite number of discrete material components. As such, they are characterized by an a priori finite-dimensional configuration space of absolute and/or relative coordinates, the relative ones being usually preferred in practice.

4) *Surrogate models:* The configuration of the system is obtained using sets of data and a learning process. The great majority of the approaches falling in this group use neural networks (NNs) models and machine learning algorithms.

This classification has been defined to ease the explanation of the models, in an effort to group them based on the different parametrization path that they employ (see Fig. 1). Clearly, this is only one of the classifications that can be conceived and, in some cases, it is possible to note some overlapping between the models that we will try to underline while going through them and which are summarized in Section X.

III. CONTINUUM MECHANICS MODELS

Soft robotics is an extremely interdisciplinary field and continuum mechanics represents the most influential community for the theoretical modeling of soft robots. Classical elasticity theories have been used for centuries to precisely model the mechanics of continuum bodies and they offer an established and general framework that is already available to the soft robotics community. Thus, one of the main goals of using these approaches in the robotics community is to make them computationally efficient for the purpose at hand, while maintaining the realism of the models produced.

In the following, we will start considering in Section III-A, the models that are obtained from the three-dimensional elasticity theory, treating the soft body as a continuum medium. We will then move in Section III-B to the so-called "director approaches" [16]. For slender bodies, these approaches are all based on the Cosserat rod theory which encompasses the Kirchhoff and the large deflections (nonlinear) Euler Bernoulli theories.

A. Classical 3-D Models

Defining a (soft) body as a set of material particles Ω labeled by their (material, in general curvilinear) coordinates $\boldsymbol{X}$, the aim of any three dimensional theory is to predict the time-evolution of its configuration $\boldsymbol{r}$ defined by

$$\boldsymbol{r}(\cdot) : \boldsymbol{X} \in \Omega \mapsto \boldsymbol{r}(\boldsymbol{X}) \in \mathbb{R}^3. \tag{1}$$

In order to proceed, the first step consists in obtaining the balance equations of the system. Shall we consider a material subpart of the body $\mathcal{B} \subset \Omega$, having frontier $\partial \mathcal{B}$ and outward unit
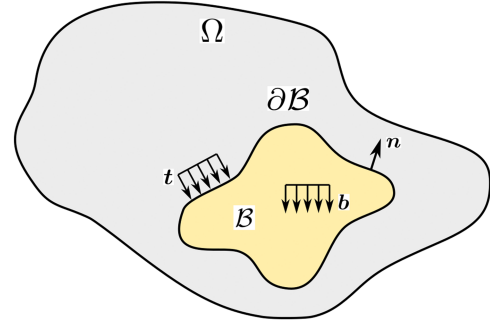

Fig. 2. Scheme of the considered body.

normal $\boldsymbol{n} \in \mathbb{R}^3$, Fig. 2. In general, volume and surface forces are applied upon $\mathcal{B}$, and modeled by some volume and surface vector densities, $\boldsymbol{b} \in \mathbb{R}^3$ and $\boldsymbol{t} \in \mathbb{R}^3$, respectively. While the first represents the external forces acting on the volume, the latter represents the forces that $\mathcal{B}$ exchanges with its surroundings (the other parts of Ω) across its boundary $\partial \mathcal{B}$, which are also known as internal forces. In particular, $\boldsymbol{t}$ is called stress vector and we admit the Cauchy theorem, i.e., $\boldsymbol{t} = \boldsymbol{\sigma} \boldsymbol{n}$, where $\boldsymbol{\sigma} \in \mathbb{R}^3 \times \mathbb{R}^3$ is the Cauchy's stress tensor. It is then possible to express the balance equations for any part $\mathcal{B}$ of Ω, as

$$\int_{\mathcal{B}} (\boldsymbol{b} - \rho \dot{\boldsymbol{v}}) \, dV + \int_{\partial \mathcal{B}} \boldsymbol{t} dS = 0 \tag{2}$$

where ρ is the mass density, $\boldsymbol{v}$ is the body velocity, and "·" denotes the partial time-derivation $\partial./\partial t$. Using divergence theorem, and remarking that (2) holds for any material subdomain $\mathcal{B}$, yields the Cauchy equilibrium equations

$$\nabla \cdot \boldsymbol{\sigma} + \boldsymbol{b} = \rho \dot{\boldsymbol{v}} \tag{3}$$

where "$\nabla \cdot$" stands for the divergence operator. In order to close the formulation, (3) needs to be supplemented with a definition of the strains and a constitutive relation characterizing the response of the body's material under external forces (or any external stimuli), i.e., a relationship between the stress tensor $\boldsymbol{\sigma}$ and an objective strain measure as the Green–Lagrange tensor field

$$\boldsymbol{E} = \frac{1}{2} \left(\nabla \boldsymbol{r}^T \nabla \boldsymbol{r} - \nabla \boldsymbol{r}_o^T \nabla \boldsymbol{r}_o \right) \tag{4}$$

where $\nabla \boldsymbol{r}$ is the gradient (the Jacobian) of the nonlinear map (1), while the index o denotes the positional field over a reference configuration. There are different ways to define a constitutive relation and the first and most famous example is the Hooke's law for linear elastic materials, which in the 1-D case reads $\sigma = E \epsilon$. One other more general constitutive relation has been proposed by Green, employing the concept of strain energy function. A Green elastic material (also known as hyperelastic material) is a type of medium for which the stress–strain relationship can be derived from a strain energy density function (or stored-energy function). This function depends symmetrically on the principal stretches (the eigenvalues of (4)) λ_1, λ_2, and λ_3, which, for incompressible materials satisfy the constrain $\lambda_1 \lambda_2 \lambda_3 = 1$. It is worth to remind that the stretch ratios λ_i

are defined as the ratio between the stretched length l_i and the undeformed one. Many soft robotics devices and components are realized with rubber-like materials, which, in the case of static deformations, are often treated as hyperelastic (while, in general, they can exhibit other nonlinear behaviors, such as hysteresis, visco-elasticity, and stress softening). Beyond Green's model, the Ogden [17] material model represents one of the most general framework for the modeling of hyperelastic materials. In such a material, the strain energy density is expressed in terms of the principal stretches of the left Cauchy–Green strain tensor $B = (\nabla r \nabla r_o^{-1})(\nabla r \nabla r_o^{-1})^T$ as

$$U\left(\lambda_1, \lambda_2, \lambda_3\right) = \sum_{j=1}^{n} \frac{\mu_j}{\alpha_j} \left(\lambda_1^{\alpha_j} + \lambda_2^{\alpha_j} + \lambda_3^{\alpha_j} - 3\right) \quad (5)$$

where n, μ_j, and α_j are material constants. In particular, for $n = 1$ and $\alpha = 2$, the Neo–Hookean model is obtained, while the Mooney–Rivlin model for an incompressible material is obtained for $n = 2$, $\alpha_1 = 2$, $\alpha_2 = -2$. Once the strain energy function is defined, the principal Cauchy stresses σ_1, σ_2, and σ_3 are related to the principal stretches through the equations

$$\sigma_i = \lambda_i \frac{\partial U}{\partial \lambda_i} - p \quad (6)$$

where p represents the Lagrange multiplier (or pressure), associated with the incompressibility constraint. It is worth to remind that the Cauchy principal stresses are related to the corresponding nominal (or engineering) stresses σ_e by the relationship $\sigma_{e,i} = \sigma_i \lambda_i^{-1}$. The great majority of the materials that are employed within the soft robotics community can be considered as hyperelastic. However, most soft robotics modeling approaches still rely on a linear-elastic material assumption, as they are mostly focused on the description of the large deformation of the body, rather than the large strains.

B. Directors Approaches

The abovementioned 3-D model applies to material bodies of any geometry (at rest). However, there are many situations where the considered bodies are flattened or elongated, i.e., where two or one of the material dimensions dominate the others. In the first case, we speak of plates or shells, in the second of beams or arches. In these cases, the full 3-D position field of (1) can be developed in Taylor series around a reference material surface for shells, or a material line for beams, and the dependence on small orthogonal material dimensions analytically preintegrated into the thickness. At leading order, this provides reduced models where the positional field r of (1) is replaced by that of the reference surface or line, plus vector fields supporting the remaining small dimensions, named *directors*. For both 2-D or 1-D reduced media, the resulting models are due to Kirchhoff and Reissner depending whether transverse shearing is neglected or not. In robotics, except for modeling soft robots inspired of octopus [18], [19], [20], the great majority of these reduced models are beam models. To obtain such models, one can advantageously replace the limit process applied to the 3-D model [16], by a simpler approach consisting in directly modeling the rod as a material line along which is continuously stacked a set of rigid
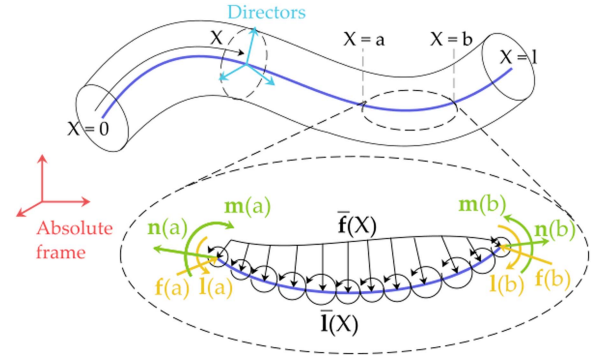

Fig. 3. Cosserat rod representation.

cross-sections (supporting the directors), and labeled by a single material coordinate X. In this case, the rod is called a *Cosserat rod* [21]) and its configuration is defined by the positional vector field $r \in \mathbb{R}^3$ of its center-line, and the orientation (rotation) field $R \in \mathrm{SO}(3)$, of its (mobile) cross-sectional basis (of directors). Both these fields are functions of $X \in [0, l]$, where l is the rod length at rest. With this parametrization, the balance equations of the rod can be derived with the Newton's law and Euler's theorem, by considering an arbitrary subinterval $[a, b] \subset [0, l]$ of the rod (see Fig. 3). Across any X-section splitting the rod in two parts, the action of the side $Y \le X$ upon the other side is modeled by the stress resultant vector $n(X)$ and the couple stress $m(X)$ in the global frame. The mass density of the rod is ρ, I is its cross-sectional inertia tensor, while v and ω are the linear and angular velocities of cross-sections in the global frame. The rod is also subject to some external forces $\bar{f}$, and moments $\bar{l}$ densities per unit of X, in the global frame. Stating the linear and angular (Newton–Euler) balance equations over the subdomain $[a, b]$, and taking the limit of the interval going to 0 provides the dynamic equilibrium [16]

$$\begin{cases} n' + \bar{f} = \rho A \dot{v} \\ m' + r' \times n + \bar{l} = \partial_t (\rho I \cdot \omega) \\ n(0) = -f_0 , \ n(l) = f_l , \ m(0) = -l_0 , \ m(l) = l_l \end{cases} \quad (7)$$

where from now on, a "'" denotes the space-partial derivative $\partial(\cdot)/\partial X$, while $l_{0,l}$ $f_{0,l}$ are the moments and forces applied in $X = 0$ and $X = l$, respectively. In order to close the formulation, (7) needs to be supplemented with a definition of strains and a stress–strain law. In the assumption of finite deformations and small strains, one can use as strain measurements the two 3×1 vectors

$$\epsilon_\ell = R^T \left(r' - r'_o\right) , \ \epsilon_a = K - K_o \quad (8)$$

where the index o denotes a reference configuration of the rod, $K = (R^T R')^\vee$ is the vector of material torsion and curvature in the cross-sectional frame, where $\vee$ changes any skew symmetric matrix $W \in \mathbb{R}^3 \times \mathbb{R}^3$ into $W^\vee \in \mathbb{R}^3$ s.t. $\forall V \in \mathbb{R}^3$, $WV = W^\vee \times V$, while conversely $\wedge$ is s.t. $\hat{W}^\vee = W$. In this context, the constitutive law takes the usual linear Hookean form

$$n = R\mathcal{H}_\ell \epsilon_\ell , bmm = R\mathcal{H}_a \epsilon_a \quad (9)$$

with $\boldsymbol{\mathcal{H}}_\ell = \boldsymbol{diag}(EA, GA, GA)$ and $\boldsymbol{\mathcal{H}}_a = \boldsymbol{diag}(GI_1, EI_2, EI_3)$ defining the usual cross-sectional linear and angular stiffness matrices in the cross-sectional frames, respectively. In the recent years, the abovementioned model has been reformulated and exploited in the modern language of Cosserat rod theory on Lie groups. Introduced in biorobotics [22], [23] to study dynamics of hyper-redundant locomotors, the configuration of a soft body is directly defined as a curve

$$\boldsymbol{g}(\cdot) : X \in [0, l] \mapsto \boldsymbol{g}(X) \in \mathrm{SE}(3) \tag{10}$$

where $\boldsymbol{g}(X)$ denotes the 4×4 homogeneous matrix of the X-cross sectional frame, with positional and rotational components denoted $\boldsymbol{r}(X)$ and $\boldsymbol{R}(X)$, respectively. The space variations of the field $\boldsymbol{g}$ can be entirely described by the field of space-twists $\boldsymbol{\xi} = (\boldsymbol{K}^T, \boldsymbol{\Gamma}^T)^T \in \mathbb{R}^6$, which defines a continuous geometric model of the rod

$$\boldsymbol{g}' = \boldsymbol{g}\widehat{\boldsymbol{\xi}}, \quad \boldsymbol{g}(0) = \boldsymbol{g}_0. \tag{11}$$

With these definitions, the strain state (9) can be expressed as a unique field of twist $\boldsymbol{\epsilon} = (\boldsymbol{\epsilon}_a^T, \boldsymbol{\epsilon}_\ell^T)^T = \boldsymbol{\xi} - \boldsymbol{\xi}_o$. Similarly, replacing X by the time variable t, yields

$$\dot{\boldsymbol{g}} = \boldsymbol{g}\widehat{\boldsymbol{\eta}} \tag{12}$$

which defines the field of velocity twist $\boldsymbol{\eta} = (\boldsymbol{\Omega}^T, \boldsymbol{V}^T)^T \in \mathbb{R}^6$, where $\boldsymbol{\Omega}(X), \boldsymbol{V}(X) \in \mathbb{R}^3$ are the angular and linear velocity of the X-cross-sectional frame in its mobile basis, which are related to their inertial counter-part through: $\boldsymbol{\Omega} = \boldsymbol{R}^T\boldsymbol{\omega}, \boldsymbol{V} = \boldsymbol{R}^T\boldsymbol{v}$. On SE(3), the dynamic equilibrium equations of a rod subject to a density of external wrench $\bar{\boldsymbol{F}}$ on $]0, l[$ and two tip external wrenches $\boldsymbol{F}_0$ and $\boldsymbol{F}_l$ at $X = 0$ and $X = l$, respectively, are expressed in the cross-sectional frames, in the form [23], [24]

$$\begin{cases} \boldsymbol{\mathcal{M}}\dot{\boldsymbol{\eta}} - \mathrm{ad}_{\boldsymbol{\eta}}^T \boldsymbol{\mathcal{M}}\boldsymbol{\eta} = \boldsymbol{\Lambda}' - \mathrm{ad}_{\boldsymbol{\xi}}^T \boldsymbol{\Lambda} + \bar{\boldsymbol{F}} \\ \boldsymbol{\Lambda}(0) = -\boldsymbol{F}_0, \quad \boldsymbol{\Lambda}(l) = \boldsymbol{F}_l \end{cases} \tag{13}$$

where ad is the adjoint action of the Lie algebra, $\boldsymbol{\mathcal{M}}$ is the 6×6 cross-sectional inertia matrix, and $\boldsymbol{\Lambda}$ models the stress field along the beam (it is the dual counterpart of the strain field). The balance (13) can be derived by applying Hamilton's principle in the framework of Lagrangian reduction theory [19], or deduced from (7), by using the relations between vectors of components in the inertial and cross-sectional frames: $\boldsymbol{\eta} = ((\boldsymbol{R}^T\boldsymbol{\omega})^T, (\boldsymbol{R}^T\boldsymbol{v})^T)^T$, $\boldsymbol{\Lambda} = ((\boldsymbol{R}^T\boldsymbol{m})^T, (\boldsymbol{R}^T\boldsymbol{n})^T)^T$, $\boldsymbol{F}_{0,l} = ((\boldsymbol{R}^T\boldsymbol{l})_{0,l}^T, (\boldsymbol{R}^T\boldsymbol{f})_{0,l}^T)^T$, and $\bar{\boldsymbol{F}} = ((\boldsymbol{R}^T\bar{\boldsymbol{l}})^T, (\boldsymbol{R}^T\bar{\boldsymbol{f}})^T)^T$. Equation (13) is first-order PDEs that govern the time-evolution of velocities $\boldsymbol{\eta}$ along the rod. Thus, they need to be supplemented with the kinematic model (12) allowing us to reconstruct (by integration) the time-evolution of the configuration $\boldsymbol{g}$.

To apply the Cosserat rod model to soft robots, an actuation model must be introduced into the abovementioned formulation. In general, this has to be done on a case by case basis, depending on the specific technology and design of the robot. However, this task has been fully accomplished in the case of tendon-driven robots. Two equivalent approaches have been proposed in this case, depending whether the effect of actuation is introduced through the densities of external wrenches $(\bar{\boldsymbol{l}}, \bar{\boldsymbol{f}})$ or through a field of internal stress $\boldsymbol{\Lambda}$ added to the elastic restoring ones of

the constitutive law (9). In both approaches, the tendons are idealized as inelastic and friction-less force transmitters. Initiated in the planar case in [25] and extended to the three-dimensional case in [26], the first approach is based on the application of the Newton's laws to the rod and to each of the tendons, isolated separately. Then, using the action-reaction principle provides the internal forces and moments exerted by a set of n_a tendons onto the rod

$$\begin{pmatrix} \bar{\boldsymbol{l}} \\ \bar{\boldsymbol{f}} \end{pmatrix} = -\sum_{i=1}^{n_a} \begin{pmatrix} \boldsymbol{d}_i \times \boldsymbol{t}'_{ci} \\ \boldsymbol{t}'_{ci} \end{pmatrix} u_i \tag{14}$$

where $\boldsymbol{d}_i(X)$ and $\boldsymbol{t}_{ci}(X)$ are, respectively, the position vector of the tendon routing i with respect to the rod's backbone and its unit tangent vector, both expressed at X, while $u_i(t)$ is the uniform tension ($u'_i = 0$) transmitted along the tendon. In the second approach [27], [28], applying the virtual work principle to the whole arm, allows modeling the effect of tendons by changing the constitutive law (9) into the active one [28]

$$\begin{pmatrix} \boldsymbol{m} \\ \boldsymbol{n} \end{pmatrix} = \begin{pmatrix} \boldsymbol{R}\boldsymbol{\mathcal{H}}_a \boldsymbol{\epsilon}_a \\ \boldsymbol{R}\boldsymbol{\mathcal{H}}_\ell \boldsymbol{\epsilon}_\ell \end{pmatrix} + \sum_{i=1}^{n_a} \begin{pmatrix} \boldsymbol{d}_i \times \boldsymbol{t}_{ci} \\ \boldsymbol{t}_{ci} \end{pmatrix} u_i \tag{15}$$

where the derivatives of $\boldsymbol{t}_{ci}(X)$ appearing in (14) are now taken in charge by the space derivations of the equilibrium equations (13).

Remarkably, other nonlinear beam theories can be defined as submodels of the abovementioned theory, often referred to as the Reissner beam model [29]. The Kirchhoff rod theory can be obtained by fixing in $\boldsymbol{\xi}$ of (11), the first component Γ_1 of $\boldsymbol{\Gamma}$ to one, and the two others to zero, which prevents the beam from stretching and shearing, respectively. By imposing that the motion of a Kirchhoff rod is planar and ignoring its thickness, the stress equilibrium (13), restricted to statics, can then be integrated explicitly. The model is then that of the *elastica*, i.e., an elastic line of minimal curvature energy, and we have

$$\mathrm{EI}(X)\theta' = M_{\mathrm{ext}} \tag{16}$$

where $\theta'(X)$ is its curvature in the plane, $\mathrm{EI}(X)$ its bending stiffness, and $M_{\mathrm{ext}}(X)$ is the integral of the external bending moments about the center of the X-cross section, acting on the remaining part ($Y > X$) of the beam.

IV. NUMERICAL RESOLUTION OF 3-D CONTINUUM FORMULATIONS

To integrate the dynamics of a soft manipulator modeled by 3-D continuum mechanics, one needs to solve for each material subdomain a closed formulation obtained by the PDEs (3) with a definition of strains, a constitutive law of the type of (6) and BCs (some of them imposed by the connection of the bodies). The usual numerical resolution methods use finite differences to discretize the time axis through explicit or implicit integration schemes. However, the spatial discretization can be achieved differently by using finite differences, boundary elements, or finite-elements method. The first approach is based on Taylor approximations of the PDEs, but it is difficult to apply to complex shaped objects, while the second is based on Green's theorems and restricted to linear problems. In contrast, the finite-elements

method has the advantage of inheriting the variational structure of the original formulation, which is transformed into a robust nonlinear optimization problem in the context of the Ritz method.

A. Finite-Element Method (FEM) for 3-D Formulations

FEM is a well-known and widely-spread numerical technique for finding approximate solutions to PDEs. It was established by a set of scientific papers in the 40 s and it soon became one of the most commonly employed technique for the modeling of a wide range of engineering problems. The main property of this technique is the subdivision of the problem's domain into a set of smaller parts, called *finite elements*. These are obtained by the construction of a *mesh* [see Fig. 1(a)], which represents the numerical domain for the solutions. Once this space discretization is performed, the continuous field r is approximated on each element by a polynomial interpolation of its values at the edges of the elements, called nodes, according to a Ritz reduction approach. Introducing this discretization in the above continuous formulation and projecting it on the same trial (polynomials) basis, changes the PDEs (3) into a set of algebraic discrete equations for steady-state problems, or ODEs for transient problems. In the former case, the static equilibrium becomes

$$Q_{\text{int}}(q) = Q_{\text{ext}}(q) \quad (17)$$

where $Q_{\text{int}}(q)$ and $Q_{\text{ext}}(q)$ represent the internal and external generalized forces, respectively, while q are the generalized coordinates, i.e., the nodal positions. On the other hand, the dynamic equilibrium is given by a system of ODEs

$$\begin{cases} \dot{q} = v \\ M\dot{v} + Q_{\text{int}}(q, v) = Q_{\text{ext}}(q, v) \end{cases} \quad (18)$$

where M is the (constant) generalized mass matrix. Note that the terms appearing in (17) and (18) are computed integrating the distributed variables element-by-element according to the selected shape functions, which play the role of the kinematic map, while the position of each element in the mesh is ensured by the assembly process. Since nodal coordinates are of absolute nature, the nonlinearities appear in $Q_{\text{int}}(q, v)$. They are named *geometric* or *material*, depending whether they come from the large displacements (and namely the rotations) of the elements, or from the constitutive laws. To capture the local finite rotations along bodies, the corotational approach is often used in three-dimensional finite element (FE) software. One other solution to represent the nonlinearities is to use an absolute nodal coordinate formulation (ANCF-FEM) [30].

The FEM represents a standard for many popular simulation software, such as Abaqus, ANSYS, and COMSOL. The main advantage of these software is that they provide a powerful and general tool that can be applied to a wide spectrum of physical problems ranging from structural dynamics, fluid-structure interactions, contact, and thermodynamics. Moreover, they provide a readymade and user-friendly framework that can be easily employed for specific studies on multiphysics systems. They have been widely used to model soft robots [31], [32]

(Abaqus), [33] (ANSYS). However, their generality intrinsically entail an increased computational cost and the simulations can take a lot of time to converge. There are some popular examples of ad hoc finite-element approaches (and softwares) that have been specifically proposed for (soft) robotics applications. In 2007 [34], a group of researchers from different institutes released simulation open framework architecture (Sofa), an open-source C++ library, which was originally presented as a computational environment for medical simulations [35], [36]. In the following years, Sofa became a comprehensive high-performance library that have been widely implemented for different application fields, and a SoftRobots plugin was also created for the design [37], modeling and control [38], [39] of soft robots, including self-collision scenarios [40]. More recently, a model combining the FEM and the discrete Cosserat approach of Section III-B was presented in [41]. A discussion on the architecture of the software is addressed in Section IX, while here we mostly focus on the modeling part for the soft bodies. In Sofa, a deformable continuum is modeled using a dynamic or quasi-static system of simulation nodes. The node coordinates are the independent DOFs of the object, and they are typically governed by equations of the type (17) and (18). Some approaches have also introduced reduced coordinates and these are presented in Section VIII-B. With regards to the actuation, a constraint-based approach is employed. Imposing a linearization of the internal forces $Q_{\text{int}}(q_i) \approx Q_{\text{int}}(q_{i-1}) + K(q_{i-1})dq$ and considering the contribution of the actuation constraints, the static equilibrium at each ith step (17) becomes:

$$Q_{\text{int}}(q_{i-1}) + K(q_{i-1})dq = Q_{\text{ext}}(q_{i-1}) + B(q_{i-1})^T\lambda \quad (19)$$

where the term $B^T\lambda$ models the contributions of the Lagrange multipliers (i.e., those of the actuators), and B represents the Jacobian of the constraint equations imposed by the actuators. The following three steps are then performed.

1) a free configuration q^{free} is found for $\lambda = 0$ and, for each constraint, the violation δ^{free} is estimated;
2) the solver computes the value of λ through a projection of the mechanics into the constraint space, obtaining the smallest possible projection space $\delta = BK^{-1}B^T\lambda + \delta^{\text{free}}$;
3) the final configuration is corrected using the value of the constraint response $q = q^{\text{free}} + K^{-1}B^T\lambda$.

For a fluidic actuation, λ and δ represent the cavity pressure and volume. For a cable, λ and δ are the cable tension and length. While in the inverse model case, λ is unknown and can be find by solving a QP type problem [36], in the direct problem case, λ can be unknown too, as this is the case of a cable driven arm where the nonnegative tensions condition is modeled as a set of unilateral and complementarity (nonholonomic) constraints. Because standard finite elements are not differentiable at element boundaries, some authors have recently implemented a moving least squares (MLS-FEM) formulation, making the deformation gradient twice differentiable [42], with the aim of applying usual optimization gradient descent techniques to different design problems related to automated actuation routing [43] and sensor design [44] for soft robots.

V. NUMERICAL RESOLUTION OF DIRECTORS-BASED FORMULATIONS

The closed formulation of a soft manipulator modeled by Cosserat rods consists, for each rod, of the kinematic model (12), the stress balance (13) (where the BCs can depend on the connection between the rods), and a constitutive law of the type of (9), with the associated strain definition (8). This formulation is consistent with the definition of the configurations (10) in terms of the absolute fields g. For soft manipulators, one can alternatively parameterize the configuration with the fields $\boldsymbol{\xi}$ or $\boldsymbol{\epsilon}$ and use (11) as a space-reconstruction equation of g along the rod. Time-differentiating twice this geometric model (11) provides two further models [23] [45]

$$
\begin{aligned}
\boldsymbol{\eta}' &= \dot{\boldsymbol{\xi}} - \mathrm{ad}_{\boldsymbol{\xi}} \boldsymbol{\eta} \\
\dot{\boldsymbol{\eta}}' &= \ddot{\boldsymbol{\xi}} - \mathrm{ad}_{\dot{\boldsymbol{\xi}}} \boldsymbol{\eta} - \mathrm{ad}_{\boldsymbol{\xi}} \dot{\boldsymbol{\eta}}
\end{aligned}
\tag{20}
$$

whose spatial integration allows us to reconstruct the absolute velocity and acceleration fields along the rod, from the strain velocities and accelerations $\dot{\boldsymbol{\xi}}$, and $\ddot{\boldsymbol{\xi}}$. In this case, the parametrization of configurations is said to be relative and opposed to the classical absolute one based on g. In this section, we discuss the most important examples of approaches using Cosserat rod's theory for modeling soft robots. They are separated into "nonenergetic" and "energetic" methods. In the first case, the original formulation is first set in the form of a space boundary value problem (BVP) with BCs partly defined at one end, and partly at the other. Then, this BVP is directly discretized on a spatial grid with no further reduction. In the second case, often referred to as the "Ritz" or "Ritz–Galerkin" method, the configuration needs first to be parameterized by some vector fields (absolute or relative) that are reduced on a truncated functional basis of space-dependent vectors. The components along these vectors define a finite set of generalized coordinates governed by a set of Lagrange ODEs in time. In the following, Ritz methods are classified into nodal and modal, depending whether the basis is defined by some nodal interpolation polynomials over the finite elements of a mesh, or defined over the full rod domain.

A. Nonenergetic Approaches

In practice, these approaches consist in extracting from the previous model a closed formulation (absolute, relative, or mixed), which is reshaped into one of the standard forms of numerical analysis.

1) Finite Differences: The finite-difference method is one of the simplest and oldest methods to solve PDEs. In the case of Cosserat beams, it has been widely used by the ocean engineering community to predict the temporal evolution of towed submarine cables, subjected to low tensions that cause a dynamic singularity in the standard catheter model. Developed by Burgess and his successors [46], [47], the direct dynamics of the cable modeled by a shear-less Cosserat rod is formulated as a nonlinear BVP in space and an initial value problem (IVP) in time. The application of a spatial finite-difference scheme transforms this continuous formulation into a set of time-ODEs at the grid nodes, which can then be solved explicitly, or by a predictor–corrector strategy (with correction by the Newton–Raphson algorithm), depending on whether an explicit or implicit time finite-difference scheme is used. In continuum and soft robotics, finite-differences method has been applied to both statics [48], [49] and dynamics [24], [50]. One canonical example of such a numerical resolution applied to soft robotics is presented in [24], where the dynamic modeling and simulation of a cable driven multibending soft robot arm is addressed. Gathering the geometric model (12), with that of velocities (20)$_1$, and the balance of stress (13), in which the model of tendons actuation (14) and the constitutive law (9) are introduced, allows first to set the forward dynamics BVP in the form $\dot{z} = \boldsymbol{f}(z, z'z,'' t)$, where z is composed of the angular and linear components of fields $g, \boldsymbol{\epsilon}$, and $\boldsymbol{\eta}$, while the time dependency is due to the actuation. Then, approximating, the space derivatives of the kinematic field $\boldsymbol{\eta}$ with a forward (from the base to the tip) finite-difference scheme, and those of the strains field $\boldsymbol{\epsilon}$, with a backward one (from tip to the base), this BVP is changed into a finite-dimensional state system of the usual form $\dot{\boldsymbol{x}} = \boldsymbol{f}(\boldsymbol{x}, t)$ that can be time-integrated with a standard explicit Runge–Kutta integrator.

2) Shooting Methods: The shooting method represents one of the most popular numerical approach to solve a BVP along one dimension of space or time. In the context of Cosserat rods, it has been introduced in the oceanic engineering community of submarine cables as an alternative way to finite differences for solving the forward dynamics of these systems [51]. In the case of soft arms, the archetypal BVP is that of the forward static model of a Cosserat rod. It is obtained by gathering (11) with the stress balance (13), in which we remove the velocities and accelerations. Then, expressing the strains in terms of stress by inverting the constitutive law (9) provides a (forward static) BVP in the form $z' = \boldsymbol{f}(z)$ that can be solved by the shooting algorithm, i.e., by integrating a sequence of initial (proximal) value problems, whose unknown proximal conditions are first predicted and then iteratively corrected (with a Newton type-algorithm), until a solution of the BVP that fulfills the known distal BCs is found [see Fig. 1(b)].

In [26], Cosserat theory is used for static and dynamic modeling of continuous robots, driven by tendons. The effect of tendons on the rod is modeled as some densities of external forces and moments defined by (14), in which the routing path of each tendon is expressed as a function of the rod strain variables. After some clever algebraic manipulations, an explicit BVP of the forward statics in the form $z' = \boldsymbol{f}(z, t)$ is obtained, to which the shooting method is applied for the purpose of calculating the static equilibrium configurations of these systems. In [52], the shooting-based resolution was extended from statics to the forward dynamics of several designs of continuum robots for simulation purposes. Inspired by [51] and [53], an implicit time-integrator is used in order to remove the time derivatives of the system of PDEs (12), (20)$_1$, and (13). Using the constitutive law (9) and the model of actuation (14), provides a BVP in space in the usual form $z' = \boldsymbol{f}(z, t)$, that is, solved at each time-step of the simulation by the shooting method starting from a prediction. With the rapid expansion of continuum robotics, the approach has been successfully extended to several multisegment designs, ranging from multisegment tendon robots [54], to parallel continuum robots [52], [55], to concentric tube robots [56] and [57].

In the first case, the BVPs along segments are connected in series by their BCs and the approach is reapplied in cascade from the base to the tip of the arm. In the second case, it is applied along each legs and the residual vector of distal conditions must integrate the equilibrium equations of the rigid platform. In the third case, the superimposed tubes must be considered as nonmaterial domains of varying length, along which the method is applied in cascade.

3) Continuous Newton–Euler-Based Method: The Newton–Euler formalism of rigid multibody systems has produced fast and simple algorithms for solving the direct and inverse dynamics of rigid robots [58]. In [22], the Luh "computed torque algorithm" has been extended to solve the inverse dynamics of fish-inspired hyper-redundant robots modeled as Cosserat rods whose shape is controlled by the internal torque field $R^T m$. Concatenating (13) with (11), and its first and second time-derivatives (20), defines a continuous Newton–Euler model, where the rod sections take the place of the rigid bodies and K that of the joint variables of a rigid discrete system. Imposing the curvature time law in this model provides an inverse dynamics BVP, which, in contrast to the forward dynamics one, can be solved in two decoupled pass (i.e., without resorting to shooting). Solving the (locomotion) dynamics of net motions, this algorithm has been extensively exploited for the study of bio-inspired swimming [59]. Although first designed for hyper-redundant systems, this algorithm has been recently applied to soft and continuum robotics [28]. Remarkably, when pose-dependent external forces (such as gravity) are neglected, the forward static BVP enjoys the same decoupling property as the inverse BVP, a feature that was exploited in [60] for quasi-static simulation of tendon-driven robots with the same two pass approach. Note that in such cases, the Newton–Euler and finite-difference-based approaches can lead to the same numerical solutions but from different points of view.

4) Collocation Methods: Alternatively to shooting, the forward static BVP of soft arms can also be solved using the collocation method. The main idea is to replace the unknown strain field with a polynomial and setting the vanishing of the residual between the two in a finite set of points on the domain, also called collocation points. Considering m collocation points, a total of $m + 1$ equations is obtained, providing the parameters that are required to define an mth order polynomial. In [61], the ODEs describing the kinematics of a Cosserat rod are directly solved in terms of transformations on SE(3), using a combination of orthogonal collocation and forward integration through Magnus Expansion on SE(3). In particular, the unknown $\xi(X)$ in (11) is expressed as a set of three Chebyshev polynomials.

B. Energetic Approaches

Energetic approaches seek to reduce the continuous models of Section III-B to a finite set of Lagrangian ODEs in time, thus retaining the variational (energetic) structure of the modeling.

1) Absolute Nodal-Ritz Reduction: One of the most powerful method to capture in an exact manner the geometric nonlinearities of soft robots is the geometrically exact FEM (GE-FEM) introduced by Simo [62]. In this approach, the model of rotations is introduced at the same level as that of positions, by replacing the material points of classical medium by the rigid microstructures of a Cosserat medium. The GE character, then imposes to apply the FEM without resorting to any simplifications on finite rotations, except the unavoidable space and time discretizations required by the numerical resolution. The GE-FEM was developed for both shells [63], and rods [64], [65], [66]. The method's tour de force was to generalize all the key operations of the FEM (interpolation and space and time-integration), from the linear vector space of positional fields to the curved manifold SO(3). Rooted in Lagrangian mechanics, the resulting dynamic equations take a form similar to that of (18), except that q and v are now defined by the sets of (r, R) and $(\dot{r}, \Omega)$ at the nodes, while an additional Coriolis term survives due to the intrinsic curvature of SO(3)

$$M\dot{v} + C(v)v + Q_{\text{int}}(q, v) = Q_{\text{ext}}(q, v). \quad (21)$$

Finally, (21) is solved iteratively at each time step according to a standard prediction–correction strategy, in which the time-dependence is removed with an implicit geometric time integrator on $SO(3) \times \mathbb{R}^3$, which preserves the Lie group structure and the geometrically exact character of the approach. This approach, which is probably the most advanced for modeling mechanisms of rods subject to rigid motions and finite deformations, is today used as a reference for others, and commercialized in the SAMCEF software through its plugin MECANO [67]. In this software, the model of rods is the full-Cosserat model of Reissner. However, its dynamic resolution is ill-conditioned when the aspect ratio of the rod increases, i.e., for very slender rods. To overcome this limitation, several FEM based on the nonlinear Euler–Bernoulli or Kirchhoff rod models, were proposed, such as the absolute nodal FEM [68] or the Kirchhoff GE-FEM [65], [69]. Despite their power, these methods have not yet been adapted to the specific needs of soft robotics as was done for Sofa. As a result, specific applications, more or less related to the original spirit of Simo's GE-FEM were proposed for these systems. In [70], a GE-FEM approach for modeling inflatable robots is presented. A strain field measuring radial inflation is added to the usual 6 strains of the Reissner model and the weak form of the static equilibrium in this augmented space is derived and solved in COMSOL.

2) Absolute Modal-Ritz Reduction: The Ritz method can be applied directly on the full domain of the rod and, in this case, we refer it to the modal-Ritz method. The approach can be applied both to absolute or relative vector fields. In the first case, one needs first to parameterize the rod configuration with a set of vector fields (e.g., the positional field along the backbone r and the vector field of its 3 cross-sections Euler's angles θ). Then, applying the separation of variables, the components of these fields can be approximated on a truncated basis of Ritz functions compatible with the BCs

$$r(X,t) = \Phi(X)q_r(t), \quad \theta(X,t) = \Psi(X)q_\theta(t) \quad (22)$$

where $\Phi(X)$ and $\Psi(X)$ are matrices of spatial shape functions, or "modes" (stacked in columns), while $q = (q_r^T, q_\theta^T)^T$ is a vector of time-dependent generalized (modal) coordinates.

In [71], the Ritz–Galerkin method is used to reduce the weak-form of a Cosserat rod in both statics and dynamics. The kinematics of the rod is obtained expressing equation (11) in an inertial reference system, placed at the base of the manipulator. Then, the positional field of the backbone can be approximated as in (22), while using Kirchhoff assumption and Bishop frames, the rotation field is parameterized with a unique further field of torsion angle. Applying (22) to this field and introducing all these approximations into the static balance equations projected onto the same truncated basis, provides a set of algebraic equations in the usual form (17). Using a numerical root finder finally provides the q_i that minimize the approximation error. In the dynamic case, applying the same reduction process provides ODEs of the form (21) where M and C depend on q due to the geometric nonlinearities introduced by the parametrization of $SO(3)$. The coefficients $q_i(t)$ are then found by explicit time-integration of these ODEs.

3) Relative Nodal-Ritz Reduction: After the works of Simo, a small group of authors proposed an alternative GE-FEM based on the polynomial interpolation of strains instead of poses [72]. This approach is more accurate, but also more computationally complex than conventional GE-FEM. In the field of soft robotics, a GE-FEM based on strain parametrization was presented in [73]. Inspired by [66], in [73], a helical shape function defined with the exponential map is used to express the shape of a manipulator. It is given in terms of the pose at the base ($X = 0$) and the strain ϵ.

4) Relative Modal-Ritz Reduction: The modal Ritz approach has been recently applied to the strain fields of Cosserat rods in the context of the geometric variable-strain (GVS) approach, [28], [74], [75]. Equation (22), thus, becomes $\epsilon(X, t) = \Phi(X)q(t)$ [see Fig. 1(c)]. In this case, the Ritz coefficients of the strains stand for the generalized coordinates of a set of homogeneous transformations along the soft robot, similar to the joint transformations for rigid ones [15]. This (relative) strain parametrization, produces a highly reduced set of ODEs in the classical form

$$M(q)\ddot{q} + C(q, \dot{q})\dot{q} + Q_{\text{int}}(q, \dot{q}) = Q_{\text{ext}}(q, \dot{q}) \qquad (23)$$

where q is then comparable to the vector of joint angles of a rigid robot. In [28], the GVS was successfully validated against the GE-FEM with standard benches in statics and dynamics. The results showed that the approach can provide very good results in terms of accuracy with a few number of generalized coordinates. Moreover, in contrast to absolute Ritz methods, the strain functions do not need to fulfill any BCs. On the other hand, unlike the usual absolute Ritz reduction (such as the FEM), it handles double space integrals which are not easy to calculate. Recent progress has been made to overcome this difficulty and obtain the reduced model (23). In [75], D'Alembert's principle of virtual works is used to project the Cosserat model (12), (13), from the space of pose fields g onto that of strain coordinates q. This approach has been achieved in a purely analytical way. It first exploits the fact that since (11) is a system of homogeneous first order ODEs of matrix form $Y' = YA(X)$, the exponential representation F of its solutions can be obtained through the

Magnus expansions, yielding to the geometric map

$$g(X) = \exp\left(\widehat{\Omega}(q, X)\right) \qquad (24)$$

where exp represents the exponential map in SE(3), and $\widehat{\Omega}(q, X)$ is the Magnus expansion of $\widehat{\xi}$, truncated at a desired order of approximation. The strain reduction and (24) are then introduced into the expressions of $\dot{\eta}$ and η obtained by analytical integration of the model of velocities and accelerations along the rods (20). This provides the kinematic map $\eta = J(q)\dot{q}$ and its time derivative $\dot{\eta} = J(q)\ddot{q} + \dot{J}(q)\dot{q}$, with $J(q)$ the Jacobian between the twist and $\dot{q}$-spaces. Finally, applying this change of space in the contributions of external and inertial forces of the weak form of the virtual works, while those of the elastic and actuation ones are directly deduced of the projection of the active constitutive law (15) on the strain modes, we obtain the EoM in the classical Lagrangian form (23). Alternatively, to this analytical Jacobian-based approach, in [28], a numerical Newton–Euler-based approach has been proposed to calculate (23). In this case, the complex double space integrals required by the strain-based parametrization are automatically performed through the two passes of the continuous computed torque algorithm of [22], whose inputs and outputs are reduced on the strain modes. In [76], the GVS approach is further extended to the modeling of concentric tube robot systems, including the modeling of the tube's insertion motion in quasi-steady conditions. In [77], the same approach is applied to the unsteady case to address the "paradoxical" dynamics of the sliding spaghetti [78]. The GVS approach has been implemented in a MATLAB Toolbox, *SoRoSim*, for the simulation of soft, rigid, and hybrid robots [75]. A special case of the GVS is the piecewise constant-strain approach (PCS) [45], [79], where the strains in the sections are assumed to be constant, an approach which has been extended to closed-chain geometries in [80]. In [81], a similar approach to PCS is presented. Based on the constant curvature (CC) assumption, it also incorporates hyperelastic and viscoelastic material behaviors. A planar restriction of the GVS, named polynomial curvature approach was introduced in [82] and [83] to address the control of planar soft manipulators. A similar approach was also used in [84] to model planar elastic flexure joints.

C. Analytical-Based Resolutions

In some specific loading conditions (especially when the rod is subject to concentrated external loads, and not distributed ones), some analytical solutions to (16) can be obtained in terms of elliptic functions. To illustrate this, let us consider the case of a simply supported beam subjected to a concentrated compressive force F applied at its tip. The analytical solution of the Euler Bernoulli equation then yields [85]

$$F = \frac{4EI}{l^2}\left[\mathcal{K}\sin\left(\frac{\theta(0)}{2}\right)\right]^2 \qquad (25)$$

where an uniform cross-section along the length of the beam is assumed, and $\mathcal{K}$ is a complete elliptic integral of the first kind. It should be noted that (25) provides an implicit expression of the base angle $\theta(0)$ as a function of the applied load F.

Once $\theta(0)$ calculated for a given F, the rotational field θ can be obtained through integration of (16), and used to get the displacement field of the rod in terms of other elliptic functions. When applicable, this approach can offer great advantages for the study of some specific phenomena related to soft robots design. EB rod theory was applied to statics and dynamics of a soft arm with a continuously rotating clamp subject to a tip dead load for the purpose of analysing snap-back phenomenon and post buckling behavior [86]. In [87], kineto-static modeling of multiple-backbone continuum robots is addressed with EB solutions able to express the deflected shapes of the backbones over a subsegment of the robot. In the paper [88], planar EB theory is applied to the modeling of continuous tendon-driven robots, and the static equilibrium of end and spacer disks is derived. In [89], EB theory is applied to the modeling of a fiber-reinforced bending actuator. The soft actuator is modeled as a Neo–Hookean material, where the strain energy functional of (5) reduces to $U = \frac{\mu}{2}(\lambda_1^2 + \lambda_2^2 + \lambda_3^2 - 3)$, with μ, the shear modulus. The principal nominal stresses are deduced from the principal Cauchy stresses of (6). Considering the fiber rein-forcement on the circumferential direction ($\lambda_2 = 1$) and the material incompressibility, provides the three nominal stress and the Lagrange multiplier p in terms of μ and λ_1. The bending moment is then deduced from stresses at the top and bottom layers, and set equal to that of the internal air pressure against the distal cap of the actuator. The actuator force is obtained from the torque balance, assuming that the actuator is constrained in a flat configuration and that no internal moments is generated under pressurization. In [90], the approach is extended in order to capture the effect of pressure on the lateral surface of the inner chamber of the actuator. In [91], a soft arm made of longitudinal pneumatic actuators is described in terms of its curvature with (16), a stretch field along the center line, and the bending plane defined by an angle at the base. The balance of internal and the external loads is then formulated, together with that of the cross section. The model is finally solved numerically, discretizing the arm into a finite number of sections and driving the residual of the static balance to zero.

VI. Geometrical Models

The main characteristic of the approaches in this section is that they rely on the assumption that the deformed shape of the soft body resemble a specific geometrical shape. All these approaches are based on a representation of the soft body which falls in the definition of a Cosserat rod. The main difference from the approaches described in Section III-B is that, when moving from the kinematics to the static and dynamic equations, these methods do not rely on the PDEs (7), but built from the generalized coordinates specifically used to represent the body geometry. We can then conclude that, while the configuration of these models can vary, being discrete or continuous, they all have their roots in some set of shape coordinates mapped to the configuration by

$$q \in \mathbb{R}^n \mapsto g(q) \in SE(3). \tag{26}$$

The equilibrium is then given by the Euler–Lagrange equations or other equivalent principles of dynamics. Note that all these approaches can be considered as some approximations of the Cosserat model starting from the model of a sequence of deformable curves. As a result, depending on their material consistency, the resulting models can be equivalent to the ones derived in the previous section, with particular reference to the Ritz-based approach of Sections V-B2 or V-B4. Two main groups of approaches fall in this category: the *functional* models and the PCC models.

A. Functional Approaches

Functional approaches probably represent one of the first attempts to model soft robotic devices. Their main characteristic is that they all use a chosen mathematical function to describe the desired space curves representing the geometry of the robot. One of the first example falling in this category is developed in [92], which employs a serpenoid curve to describe the kine-matics of snake-like robots. Then, the kinematics of the robot is obtained by simple forces and torques equilibrium, considering the action of the ground on the robot and the internal force components [93]. One other important example is the so-called modal approach that have been originally presented for the modeling of hyper-redundant robots both in statics [94] and in dynamics [95], while a survey of the approach is presented in [7]. The central concept of the approach is that of "*backbone curve*," i.e., a 3-D curve r parameterized by the integral representa-tion $r(X, t) = \int_0^X \lambda(s, t) t(s, t) ds$, where $\lambda(X, t)$ represents a length scaling factor, while $t(X, t)$ is the unit tangent vector, parameterized by any spherical kinematics representation (e.g., Euler angles, quaternions). In words, the deformed axis of the robot is represented as a curve growing along a direction field $t(X, t)$ from the base to its tip, with a magnitude rate $\lambda(X, t)$. In order to obtain the complete description of the robot geometry, the curve is equipped with a set of orthonormal frames and a roll distribution that describes the twist of the robot. At the end, the robot geometry is defined by a reduced set of shape functions, describing the backbone curve itself and a model of the twist. In [94], a set of four independent shape functions $S_i(X, t) = \{\lambda(X, t)\ \theta(X, t)\ \phi(X, t)\ \psi(X, t)\}$ is used, in which $\theta(X, t)$ and $\phi(X, t)$ are the two angles defining $t(X, t)$ and $\psi(X, t)$ is the roll distribution function. The inverse kinematic problem then consists in finding the set of shape functions satisfying the task constraints, which are usually represented by the end-effector positioning. For this purpose, a modal approach is employed and each $S_i(X, t)$ takes the form $S_i(X, t) = \sum_{j=1}^{N_{S_i}} \Phi_{ij}(X) q_{ij}(t)$, where q_{ij} are modal participation factors and the $\Phi_{ij}(X)$, N_{S_i} modal functions, which are chosen by the robot programmer to fulfill the task constraints. At the end, the robot shape is fully de-scribed by the modal factors q_{ij}, which represent the generalized coordinates of the system q in (26). In [6], it has been proved that, when the curvature of the body is assumed to be constant, this approach provides a transformation which is equivalent to (27), presented in the following section. In one other work by the same authors [7], variational approaches are presented in order to compute the optimal curve shapes that comply with both

joint and task constraints. The same kinematic model was also employed in [96] and extended to the dynamical modeling of coiling continuum robots. Another possible function that can be used to represent the robot geometry consists in the pythagorean hodograph curves [97]. The backbone is represented using quadratic polynomials, which are functions of the chosen control points, representing the generalized coordinates of the system. In order to obtain the optimal quadratic polynomials to compute the control points, the minimizing of the potential energy is applied. Finally, an NN model is employed to predict the effects of loads on the position of the robot, including the case of variable loads. In [98], the kinematics of a soft pneumatic actuator is modeled representing its backbone with cubic Hermite splines (also called cspline). In this way, the backbone is defined by two control points and two control orientations (vectors). The control points are obtained experimentally and an optimization procedure is carried out to fit the cspline with the given backbone. To complete the description of the robot configuration, the orientation along the curve is finally obtained assuming the minimizing of the torsion of the actuator's backbone. In [99], the backbone of tendon driven continuum robots is represented as a sequence of Euler arc splines, which are directed arcs whose curvature varies in arithmetic progression. This article represent an example of a modeling technique that is based on the CC assumption, as the models presented in Section VI-B, but employs a functional representation of the robot's kinematics. In [100], elliptic Fourier descriptors are employed to describe soft deformable morphologies. Compared to the other methods described in this section, this approach does not model the soft robot through its backbone, but uses a closed curve to represent the boundary of the 2-D regions that it occupies. This is obtained thanks to elliptic Fourier descriptor, through a procedure that fits a closed curve to a set of 2-D points with arbitrary precision. In particular, the image of the region occupied by the robot is extracted from experimental recordings and its contour is identified through a discrete representation. Finally, the coefficients of the Fourier series are computed, providing the description of the shape.

B. CC Models

CC is often viewed as a desirable characteristic in continuum robots, due to the simplifications it enables in kinematic modeling as well as in real-time control and other useful computations. This is motivated by the fact that actuators with a path parallel to the mid-line on a cylindrical manipulator produce a CC shape, in the absence of external forces. For these reasons, the CC assumption has been successfully applied in a great number of continuum robots modeling approaches. In these models, a soft body is represented by a finite number of circular arcs, each having a curvature that is constant in space. The coordinates q in (26) are specifically obtained to describe the circular arcs geometry. We can distinguish two main groups of PCC approaches: the *Kinematics-based models* are developed from a kinematical relation between the actuator and the arcs parameters, while the *mechanics-based models* are based on the mechanical description of the problem. Finally,

a survey on some of the main PCC approaches can be found in [6] and [8].

1) Kinematics-Based CC Models: Once the continuous body is represented as a finite set of CC segments, each of these can be represented by a finite set of arc parameters and it is possible to obtain a map from them to the task space of the robot. Different parameters can be used to describe a CC segment, yielding to different kinematics maps. One of the most popular sets of arc parameters that have been proposed consists of triplets of curvature κ, the angle of the plane containing the arc ϕ, and arc length l, which define q in (26). Different approaches have been proposed to obtain the kinematic map from these arc parameters. In [6], it has been proved that they all provide an identical transformation from the arc base to any point $s \in [0, l]$ of the robot arm (noting $\cos = \mathrm{c}$ and $\sin = \mathrm{s}$)

$$\boldsymbol{T}(\kappa, \phi, s) = \begin{bmatrix} \mathrm{c}\phi\mathrm{c}\kappa s & -\mathrm{s}\phi & \mathrm{c}\phi\mathrm{s}\kappa s & \frac{1}{k}\mathrm{c}\phi(1-\mathrm{c}\kappa s) \\ \mathrm{s}\phi\mathrm{c}\kappa s & \mathrm{c}\phi & \mathrm{s}\phi\mathrm{s}\kappa s & \frac{1}{k}\mathrm{s}\phi(1-\mathrm{c}\kappa s) \\ -\mathrm{s}\kappa s & 0 & \mathrm{c}\kappa s & \frac{1}{\kappa}\mathrm{s}\kappa s \\ 0 & 0 & 0 & 1 \end{bmatrix}. \tag{27}$$

One way to obtain (27) is based on the use of Denavit–Hartenberg (D–H) parameters [101], [102], [103].

In [101], under the CC assumptions, the continuous backbone of the robot is fitted with a virtual conventional rigid-link manipulator and modified D–H parameters are obtained to consider the coupling imposed by the curvature in a continuum system, providing the standard homogenous transformation matrix (27). In a following work [102], a similar, improved, approach is presented, finally providing the transformation from three parallel actuating tendons to the arc parameters:

$$l = \frac{l_1 + l_2 + l_3}{3} \, , \phi = \tan^{-1}\left(\frac{\sqrt{3}}{3}\frac{l_2 + l_3 - 2l_1}{l_2 - l_3}\right)$$

$$\kappa = \frac{2}{d}\frac{\sqrt{l_1^2 + l_2^2 + l_3^2 - l_1 l_2 - l_1 l_3 - l_2 l_3}}{l_1 + l_2 + l_3} \tag{28}$$

where $(l_1, l_2, l_3)^T$ are actuator's lengths, while d is the distance from the center of the section to the actuator. This approach has been applied for the modeling of a great number of continuum robots [104], [105] and [106], [107].

One of the main restrictions of these PCC models is that the used parametrization and kinematic maps can implicitly provide a numerical singularity that occurs when the curvature tends to vanish ($\kappa \to 0$), resulting in an infinite or undefined radius of curvature. In order to overcome this limitation, different solutions have been introduced. In [108] and [109], the rotational and position components of the homogeneous transformation (27) are represented in modal form, similarly to the models presented in Section VI-A. In particular, the entries in (27) are numerically approximated using multivariate Taylor series expansions for actuator's lengths variables at $\mathbf{0}$. Based on this formulation, a Lagrangian approach was developed in [110] and [111] for the spatial dynamics of a single section continuum arm and this was further extended to multisection arms in [112]. Other approaches have been mostly focused on the definition of

a different parametrization and transformation map to describe the geometry of the soft bodies. One alternative is provided by the exponential map of [113], [114], and [115]. In particular, (27) can be obtained using the exponential coordinates from the lie group theory seen in Section V-B. Considering that the transformation for a circular arc is the composition of a rotation ζ_{rot} with an in-plane ζ_{inp} transformation, one has

$$\boldsymbol{T}(\kappa, \phi, s) = \exp(\hat{\boldsymbol{\zeta}}_{\text{rot}}\phi)\exp\left(\hat{\boldsymbol{\zeta}}_{\text{inp}}(\kappa)s\right). \qquad (29)$$

In [114], this approach is applied to the modeling of concentric tubes robot. It is assumed that the two tubes have the same stiffness and are torsionally rigid, while applying torques to one another. Given the arc assumption, these torques can be considered to be uniform. The in-plane bending model is obtained employing EB linear equation and the resultant curvature of two overlapping tubes is obtained through a force balance in analogy with linear springs connected in parallel. Finally, the mapping from the arc-parameters to the Cartesian poses of the tube cross-sections is obtained with (29). Similarly, in [116], the arcs are expressed with an axis-rotation parametrization. The origin of the axis $\boldsymbol{\omega}$ is positioned at point $\boldsymbol{\rho}$ on the horizontal plane at the base of the section and $\boldsymbol{\omega}$ is perpendicular to $\boldsymbol{\rho}$. $\|\boldsymbol{\rho}\|$ is the radius of arc curvature, while $\|\boldsymbol{\omega}\| = l/\|\boldsymbol{\rho}\|$ is equal to the angle between the proximal and distal positions when $\boldsymbol{\rho}$ is used as the vertex of the angle. The CC arc is then parameterize by $(\boldsymbol{\rho}, l)$ or equivalently $(\boldsymbol{\omega}, l)$ which defines $\boldsymbol{q}$. The forward kinematics can, thus, be obtained through the exponential maps. Straightforward geometry finally provides the mapping between the configuration parameters and the length of the actuating tendons (28). In essence, this is a screw theory method, since $\boldsymbol{\omega}$ is exactly the axis of the screw motion required to cover the arc bend, as shown in [27].

One other example of a parametrization that does not entail the singularity in the proximity of a null curvature configuration is provided in [117], where for each CC section composing the robot, the configuration of a segment is defined as linear combinations of four arcs included in the section's volume. In particular, given the difference in length between opposite arcs, $\Delta_{x,i}$ and $\Delta_{y,i}$, through geometrical considerations, it is possible to obtain a transition map from the "*conventional*" arc parameters (κ, ϕ, l) and the new parametrization $(\Delta_x, \Delta_y, \delta l)$, where δl represents the change in the length of the section with respect to the at rest position. Algebraic steps are finally used to obtain the explicit expression of the analogous of (27), in terms of the new parameters.

2) Mechanics-Based CC Models: Some authors have sought to draw mechanical consequences, by applying static laws to a soft arm whose shape is described by the PCC. In [25], both the forward and the inverse kinematics for a tendon driven manipulator with parallel routines are derived in this way. More precisely, considering a single tendon that can experience only a constant tension u along its length, force, and moment balances are used to define the internal reaction forces acting on a section of the beam. This model is then extended to consider the presence of a finite number of tendons, based on an analogy with a system of linear springs acting in parallel. In the considered planar case,

the generalized coordinates $\boldsymbol{q}$ describing the configuration of the arm are the curvature κ and an axial stretch measurement ϵ_a. The static equilibrium leads to the description of the mechanical response of the manipulator in the form $\boldsymbol{Kq} = \boldsymbol{B}^T\boldsymbol{u}$, where $\boldsymbol{B}^T$ represents the tendon moment arms and the axially directed tangent. Relating the tendon tension and displacements is then possible to obtain the mechanical response of the tendons in terms of their displacements $\boldsymbol{y}$, $\boldsymbol{y} = \boldsymbol{C}_m\boldsymbol{u}$, where $\boldsymbol{C}_m$ is a compliance matrix, which is function of $\boldsymbol{B}^T$ and of the manipulator and tendon stiffness matrices and lengths. Finally, this yields to

$$\boldsymbol{y} = \boldsymbol{A}^\dagger\boldsymbol{q} \qquad (30)$$

where $\boldsymbol{A} = \boldsymbol{K}^{-1}\boldsymbol{B}^T\boldsymbol{C}_m^{-1}$ is the forward kinematics transformation matrix. Equation (30) provides a mechanics-based relationship between the beam and the tendon configuration, analogous to transformations (28). In a following work [118], the 3-D static model is also developed.

In [119], the statics of a braided pneumatic continuum manipulator is addressed. In this case, the effect of cross-sectional deformations on the arm deformation is studied using a strain energy function based on the Cauchy–Green stretch. The study shows that the PCC parametrization fails while releasing the PCC constraints gives better results. Another source of mechanical inconsistency in the PCC is related to the modeling of torsion, which is absent from the model mainly concerned with bending. In order to solve this issue, several developments of the PCC were proposed. In [120] and [121], the virtual power method is used to obtain the TDCRs robot dynamics. The considered robot geometry is that of [88], i.e., an elastic backbone connected by rigid disks and three tendon cables. The disks are considered rigid, while the backbone and the cables subsegment are treated as circular arcs. The relative pose of two adjacent discs is obtained from the two constant orthogonal curvatures (β, γ) and an additional lumped torsional angle ϵ of the subsegment, which define the $\boldsymbol{q}$-vector.

The torsion model has become particularly critical in continuum robotics of CTR, where it is at origin of the so called "snapping" phenomenon. In [122], the authors provide first the design conditions necessary for the validity of PCC approach, and conclude with a general model for CTRs. In this further model, the relative twist angle between two tubes is defined as a function of the arc length and then used to write the moment equilibrium and to impose the compatibility equations, enforcing the coincidence of the tube centerlines. The torsional strain is then deduced from the Cosserat rod equilibrium (7). The resulting BVP was then solved by exploring the entire input–output set. Based on this model, the stability analysis was performed in [123] and [124].

VII. DISCRETE MODELS

In this section, we discuss the approaches where the configuration of the system is discrete from the very beginning (i.e., the system is not discretized at the resolution level or through some assumptions on its backbone's geometry). In particular, we can distinguish the following three main groups: the lumped-mass, the pseudorigid, and the discrete rods models.
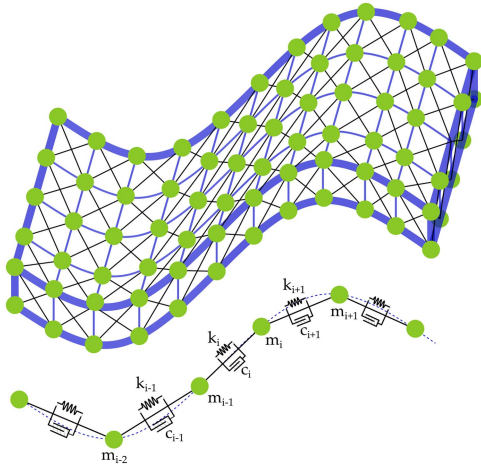
Fig. 4.   Lumped mass representation of a continuous rod.

A. Lumped-Mass Models

One of the simplest approaches to modeling a continuous body is to represent it as a set of discrete masses, dampers, and springs (see Fig. 4). The governing equations can be obtained by energy methods or applying classical Newton equations to describe the propagation of the forces from one particle to the other in the configuration space

$$Q \subset \mathbb{R}^3 \times \mathbb{R}^3 \times \mathbb{R}^3 \cdots \times \mathbb{R}^3. \tag{31}$$

The main advantage of lumped-parameter mechanics models is that they are characterized by a simple structure, easy to adapt to the capture of complex phenomena, such as nonlinear friction, material hysteresis, and inertial dynamics. On the other hand, to reach the same fidelity of the continuum mechanics models or FEM, they require a high number of DOFs and a data-expensive system identification procedure.

In [125], mass-spring-damper arrays are used to model the large deformations of a continuum surface (LDCS) actuated by continuum arms. In particular, the 3-D problem of a system composed of two interconnected layers of LDCSs is considered, where bending and shear deformations are allowed. The surface is modeled as a lattice where the masses are defined as the nodes of the system and they are connected through linear spring and dampers. Assuming a uniformly stiff surface, the elastic constant of the springs and the damping coefficients are assumed to be constant. Considering an isotropic linear elastic material, the EoM for each mass is obtained by combining direct application of the Newton's second law and Hooke's law. In [126], a lumped-mass approach is presented for the modeling of tendon driven medical robotic catheters. The axial and the bending stiffness of the model are adjusted through the selection of the spring stiffness and their radial location, while the smooth motion of the catheter is modeled through the dampers. Because of their simplicity, lumped mass models are particularly suited for large robotics simulations library, such as the one presented in [127]. Titan is a GPU-accelerated C++ software library for the modeling of soft bodies and multi-agent robots at massive scales. The main benefit of this approach is the possibility to

perform parallel computing, resulting in good computational performances.

B. Pseudorigid Models

The opportunity to exploit established rigid robotics theories for soft robots motivated the family of models that are described here. The soft bodies are represented as series of rigid links, which are connected by revolute, universal, or spherical joints [see Fig. 1(d)]. Thus, the configuration space of the soft body is given in the form

$$Q \subset \mathrm{SE}(3) \times \mathrm{SE}(3) \times \mathrm{SE}(3) \cdots \times \mathrm{SE}(3). \tag{32}$$

While these approaches can provide satisfactory results for the modeling of hyper-redundant or snake-like robots, when dealing with continuous elastic structures they provide a low order of spatial approximation accuracy, in addition to the expensive identification procedure. In [128], a dexterous catheter manipulator is represented as a series of pin joints connected by rigid links. In [129], a pseudorigid 3-D approach is applied for the modeling of a steerable ablation catheter. The catheter is treated represented as four rigid links connected by three revolute joints and three torsional springs. Venkiteswaran et al. [130] presented a pseudorigid model for continuum manipulators subject to multiple external loads. In this case, a flexible manipulator is represented as four rigid links of given length, which are connected by three joints having 2DOF each. In [131], a flexible beam is represented as a mass-less rigid body with a torsion spring attached at one end, providing the dynamical modeling of compliant mechanisms. In [132], the modeling of hyperflexible manipulators is addressed using a serial rigid chain, where the number of kinematic DOF goes to infinity. The backbone curve is first described as a continuous curve with extended Frenet frames attached to each point along its length. For the numerical simulations, the backbone curve is approximated by a serial chain of rigid bodies. In [133], a steering catheter is represented as a combination of three sections: the virtual base of the distal shaft, represented as a prismatic joint; the bending section of the distal shaft, represented as two revolute joints, one prismatic joint and two revolute joints; the distal end of the catheter, which is treated as a rigid body. In [134], a pseudorigid approach is proposed for modeling an octopus inspired swimmer. In particular, each arm of the octopus is modeled as a kinematic chain of cylindrical rigid segments, which are connected by planar rotatory joints. The first joints in the chain, connecting the arms to the main body, are modeled as actuated rotatory joints, while the other joints are modeled as (unactuated) rotatory linear spring and damper elements.

C. Discrete Rods

The computer graphics research community represents an important source of inspiration for soft robotics modeling. This is the case of the approaches that are described here, which are all based, with different extent, on the discrete elastic rod (DER) approach, originally introduced in [135], [136], and [137]. In this formulation, the inextensible Kirchhoff rod assumptions (9) are
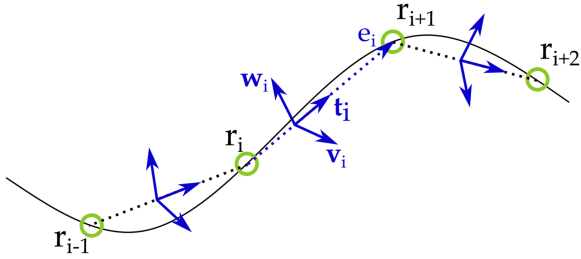
Fig. 5. Representation of a rod in the DER approach.

Fig. 6. Scheme of an NN.

considered and, similarly to the Cosserat rod model, the configuration g of an elastic rod is given by a curve $r(X)$, representing the centerline, and a material frame, where the first axis is always tangent to the curve. The Bishop (natural) frame $\{t, v, w\}$ is then introduced, providing, for a given centerline, the most *relaxed* frame, i.e., with zero twist. Finally, parallel transport allows us to define the evolution of the Bishop frame along the mid-line. This model provides a simple parametrization of the cross-sectional poses, given by the curve $r(X)$ and an angle $\theta(X)$ between the Bishop and the cross-sectional frame. The rod is then discretized into a series of finite nodes (or vertices) connected by straight segments (or edges). Each node is characterized by a position vector r_i, while each segment is associated to the edge vector $e_i = r_{i+1} - r_i$ and its tangent unit vector t_i (see Fig. 5). In this way, the discrete curvature associated with the ith vertex takes the form

$$\kappa_i = \frac{2 \sin \phi_i}{1 + \cos \phi_i} = 2 \tan \frac{\phi_i}{2} \qquad (33)$$

where ϕ_i represents the turning angle between two consecutive edges. Each ith vertex is also characterized by a total mass M_i, which is the average mass of the edges meeting in the vertex, while the mass moment of inertia for each edge can be obtained through volume integration. Finally, a discrete bending energy and a discrete twist energy can be obtained in terms of the generalized coordinates (r_i, θ_i, ϕ_i).

Following the DER formulation, in [138], the three-dimensional space of a soft filament is represented by a set of vertices $r_i(t)$ and a set of material frames $R_i(t)$. Each vertex is characterized by a linear velocity, a concentrated mass, and a set of concentrated external forces. Extension, shear and axial deformations are considered. Finally, through the spatial integration, the discrete governing equations are obtained and they are solved using a symplectic, second-order scheme. Similarly to other approaches, the external physical interactions are included in the external forces and moments vectors, while the internal physical effects (such as those modeling muscular activities) are added to the internal forces and moments resultants. In a recent work [139], this model has been implemented in an open-source simulation environment, *Elastica*, for the modeling and simulation of the dynamics of slender rods.

In [140], the planar case of the DER formulation is considered, where the rod is free to move on a plane, while the torsional deformations are neglected. Moreover, the notion of folding for a straight rod is introduced to apply the approach to
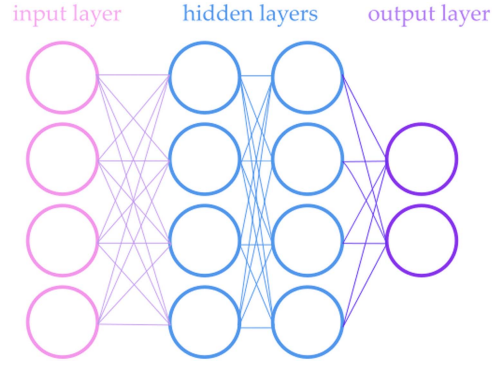
tree-like architecture, which are frequently encountered in the soft robotics community. In [141], the DER-based formulation is further enhanced to include frictional contact, inelastic collisions and inertial effects. In particular, considering a planar case, a Rayleigh damping matrix is defined to formulate the internal damping forces vector, which is added to the external forces. In order to model the contact and the friction between the robot and an unstructured ground, whose normal direction can vary with the horizontal axis, a Coulomb law is employed. In [142], the DER is hybridized with a pseudorigid body model is used to represent compliant mechanisms. Based on this model, the authors provided a computational design tool to perform different optimization tasks related to soft robotics.

VIII. SURROGATE MODELS

With respect to the models presented so far, a complete different approach to tackle the modeling of a soft robot consists in using large sets of data that are derived from various forms of external sources. These approaches are often referred to as *surrogate* or *data-driven* models and a survey on some of them is presented in [9] and [10]. While one of the main benefits of these solutions is that they do not require a physical model, on the other hand they rely on large amounts of representative data that are sometimes difficult to collect.

A. Neural Networks

NNs have been proved to be an effective tool to solve many kinds of nonlinear problems in different application fields, including robotics. As the name suggests, they are inspired from the biological NNs that operate animal brains: the artificial neurons, which represent the elementary units of NNs, can transmit a signals to the other neurons. The signal is usually a real number and the output of each neuron is computed as a nonlinear combination of all the inputs. Neurons are connected by edges and they are all characterized by weights adjusted during the learning process. Usually, neurons are gathered in layers: the first layer is also called *input layer*, the last one is called *output layer*, and the intermediate layers are called *hidden layers* (see Fig. 6). NN results in a high dimensional set of nested functions

$$y = f_M \left(A_M, \ldots f_2 \left(A_2, f_1 \left(A_1, x \right) \right) \ldots \right) \qquad (34)$$

where x are the values of the input nodes, A_i are the edges weights, f_i are the activation functions, and y are the values of the output nodes. In most soft robotics applications, the input and the output layers represent the actuation variables u and the shape parameters q. The learning process results in an optimization over the network weights, which is performed through back-propagation, a form of chain rule, where, after each forward step through the network, a backward pass is performed to compute the network Jacobian and to adjusts the model's weights accordingly. NNs have been used to approximate the kinematics, the statics and also the dynamics description of soft robots. Typically, Feed-forward neural network (FNN) are employed for kinematics and static modeling. On the other hand, recurrent neural networks are usually preferred for dynamical modeling.

The first examples of the employment of NN algorithms for the control of continuum robots were presented in [143]. In particular, a controller for continuum robots uses an FNN component to compensate the dynamic uncertainties of the system, in an attempt to reduce the uncertainty bound. In [144], the forward kinematic modeling of a bionic assistant trunk is obtained through multilayer perceptron (MLP) and radial basis function (RBF) NNs, which are both class of FNNs. The input neurons propagate the input variables to the following layers, while each neuron in the hidden layer is associated with an RBF kernel (usually Gaussian). The data are obtained experimentally, measuring the arm's tip position at varying the actuation pressure, using a trilateration algorithm. In one other paper by the same authors [145], the same handling assistant trunk is modeled, both with a data-driven and a pseudorigid modeling approach. With regards to the latter, the trunk is modeled as a series of rigid vertebrae connected by a total of four prismatic joints. For the data-driven approach, a modified Elman NN is employed. FNNs are also employed in [146] and [147], which deal with the inverse *kinetics* of a cable driven soft manipulator. While the *kinematical* model describes the configuration of the robot without considering the involved loads, the *kinetics* model relates the motion of the robot with its actuation forces. The direct kinetics model is obtained using a geometrically exact model [60]. Thus, an FNN, taking the tip position as an input and giving the cable tension as an output, is employed. An experimental data collection phase is carried out, using a set of cable tensions and obtaining the tip position with an infrared vision system. These data were used for the optimization and training of the FNN. After the training phase, the performance of the FNN is measured on test sets, using the output of the FNN as the input of the direct kinetics model. One other example of a machine learning formulation for the global inverse kinematics of continuum manipulators was presented in [148]. The data samples are generated by continuous motor babbling and a single hidden-layer artificial NN is employed to learn directly the mapping $(x_{i+1}, q_i) \mapsto q_{i+1}$, where x is the pose of the end effector. In [149], a dynamic model for open-loop control of soft robotics manipulators is presented. The PCS model described in Section V-B4 is employed to obtain the dynamics of a cable driven robot operating underwater. Considering the case where the robot and the task space have the same number of DOF, the forward dynamics of system (18) is formulated using only the task space variables and the direct mapping between the states of the task space variables and the control inputs can be obtained. Once the training is completed, an open-loop predictive controller is developed through a trajectory optimization that is carried out with an iterative sequential quadratic programming. In [150], the closed-loop controller is also implemented. The inverse kinematic modeling of a bionic trunk is addressed in [151]. In particular, a learning phase is carried out considering a volume of desired cartesian position for the robot's tip, defining a finite set of target vertices. The inverse model is asked to estimate a posture that allows us to move the effector to each vertex, and the training is carried out until the distance between the target and the actual position for each vertex is minimized.

B. Data-Driven Order Reduction

Some modeling tools employ different forms of data-driven order reduction to efficiently approximate the physical model. In [152], a Koopman operator theory is employed for a data driven controller of soft robots. A dynamical system is represented in an infinite function space $\mathcal{F}$, which is composed of real-valued functions inside the state of the system domain [153]. The elements $q \in \mathcal{F}$ are called observables. The Koopman operators, denoted by $\mathcal{U}_t$, are defined as the linear transformation $\mathcal{U}_t q = q \circ T_t$, where $\circ$ indicates the composition operation, while T_t is the flow (or dynamic) map of the system. In other words, the Koopman operator lifts the dynamics of the system from the state space to the space of the observables, describing the evolution of the observables q along the trajectories of the system. Its main advantage is that it provides a linear representation of the flow of a nonlinear system, but in the infinite-dimensional space of the observables. The discrete approximate of the Koopman operator can be obtained from a set of experimentally measured state, given in the form of snapshot pairs. Some approaches have been focused on the model reduction of FEM that were presented in Section IV-A. Model reduction methods are based on the projection of the FE EoM to attractive subspaces of smaller dimensions. In this way, the size and the computational time of the simulation are drastically lowered, allowing the application of FE methods for control purposes. In [39], a snapshot proper orthogonal decomposition is employed to generate relevant bases to be used for the order reduction. More into details, the solution q of (19) is expressed as a truncated expansion of orthonormal vectors, which depend on the constraints λ. The orthonormal basis is then set to minimize the sum of all the errors that are generated by the projection of the exact solution onto the basis. In [154], this approach is further extended for the development of a low-order controller and observer, while in [40], it is applied for the reduction of self-collision contact forces. One other example of an FE order reduction is presented in [155] for modeling soft robots made of hyperelastic materials and actuated by cables or tendons, with a special focus on contact problems.

IX. SOFTWARE IMPLEMENTATION

An important aspect of the above models and their numerical resolution, is related to their software implementation. There

TABLE I
SUMMARY OF THE MAIN MODELING FAMILIES, THEIR FUNDAMENTAL PROPERTIES, AND THEIR DESIGN APPLICATIONS

TH. BACKGROUND		REDUCTION	GEN. COORDINATES	DESIGNS	USES
CONTINUUM MECHANICS MODELS: the discretization and/or reduction is applied at the numerical resolution level.	3-D	FEM, ANCS-FEM, MLS-FEM	configurational fields values at the nodes	They can be applied to a **vast number of problems**, including 2-D and 3-D designs and actuation forces involving 3-D problems (ballooning actuators and electroactive polymers), which are modeled as constraints. On the other hand, they do not appear as the optimal solution for systems which can be modeled by ad-hoc reduced theories.	Thanks to commercial software adapted to 3-D multiphysics contexts, they can be used **to design new soft robot concepts**. They are computationally expensive and provide models with a huge number of dofs **not adapted to control and fast simulation**. Sofa is today the optimal trade-off between accuracy and computational efficiency for 3-D soft robotics. They require additional reduction treatments, to be used for control purposes.
	Directors	ABS. NODAL-RITZ	strain field values at the nodes	They provide the most efficient techniques for **1D problems mostly characterized by bending deformations**, i.e. systems that can be described as (combination of) beams and that do not involve large cross-section inflation **Thread-like actuators actions** are simply added as external or, sometimes, internal wrenches. On the other hand, they struggle in the modeling of other forms of actuation that involve 3-D problems. Relative parametrizations such as the **GVS approach** can be easily extended to hybrid soft-rigid systems. When the circular arcs assumption holds, they reduce to **mechanically consistent and singularity free PCC**.	GE-FEMs are fast and accurate for systems made of beams and rigid bodies, but are difficult to implement. In principle, other directors approaches are as accurate as GE-FEM. Energetic approaches based on modal Ritz reduction, provide **highly reduced models** in explicit standard forms, **well suited for control**. Absolute variables are more difficult to reduce than relative ones. Non-energetic approaches based on **shooting resolution**, are tailored for **real-time simulation**.
		REL. NODAL-RITZ			
		EULER BERNOULLI	bending angle function		
		NONENERGETIC	not available		
		MODAL RITZ	spatial coefficients of strain or configurational fields		
GEOMETRICAL: the backbone is represented by a specific geometrical shape.		FUNCTIONAL		PCC approaches are a specialization of GVS. They are only valid when **the circular arcs assumption holds**, i.e. in specific conditions of external and actuation loading. Similarly, functional approaches are built around a reference curve and they struggle in modeling situations which divert from this assumption.	When applicable, they are **ideally tailored to kinematic control** and offer explicit analytic maps between actuation and configuration spaces. Functional approaches often struggle to model torsion in a consistent manner.
		PCC	arc parameters or tendon lengths		
DISCRETE: the material model is a priori discretized		LUMPED MASS	mass positions	These are applications of traditional rigid theories and, for this reason, they are particularly simple and useful when applied to **hybrids systems**, combining soft and rigid components of arbitrary geometries. On the other hand, they struggle in the modeling of aspects that are more specific for soft robotics applications, such as the constitutive equations or the modeling of distributed actuation.	They are conceptually simple to implement. However, like FEM, they handle a large number of discrete dofs, **requiring reduction techniques to produce models suitable for control**. They suffer from an **inconsistent discretization**, especially for internal strain energy.
		PSEUDORIGID	joint coordinates		
		DISCRETE RODS	configurational fields values at the edges	Their applicability is comparable to that of absolute nodal Ritz methods based on directors' approaches, such as GE-FEM. They are well suited for beam and rigid body systems. They are easier to implement than FEMs, but still need to be adapted to soft robots.	Unlike other discrete approaches, they rely on a consistent discretization of the Cosserat model, based on discrete differential geometry. They have been developed for **fast interactive simulation** in computer graphics and should be **adapted to real-time simulation and control** of soft robotic.
SURROGATE: the model is obtained by regression of a large sets of data.		NNS	not applicable	They are **physics-agnostic** approaches that can be possibly applied to any design and scenario. However, the resulting models are not generalizable to new designs and conditions.	They generate **dedicated algorithms** that can be used for **fast simulation and control**.
		ORDER REDUCTION	depend on the reduction		

are several industrial as well as open-source soft robotic software/toolboxes available. Here, we briefly summarize the most popular ones. In Section IV-A, we introduced Sofa, one of the earliest open-source platforms for physics-based simulation. Its SoftRobots plugin employs a multimodal description of a problem, allowing the presence of several representations (mechanical, thermal, and visual) of the same object. This multimodal representation allows the simulation of scenarios involving the interaction of different components (rigid and/or soft bodies, fluids). PyElastica is the Python implementation of Elastica [139], described in Section VII-C. SoRoSim [75] is a MATLAB toolbox that uses the geometrically exact PVS model described in Section V-B4. One other example of a MATLAB toolbox is TMTDyn, which employs discretized lumped systems with reduced-order models [156]. SoMo (Soft Motion) [157] couples the pseudorigid model discretization of Section VII-B with a rigid body physics engine of Python to model soft robots. ChainQueen [158] and incremental potential contact simulator (IPC-Sim) [159] are simulators oriented toward computer graphics rather than mechanical systems. ChainQueen is a Python toolbox that uses the moving least square material point method, a hybrid Eulerian/Lagrangian FEM, which uses both particles and grids to simulate soft bodies. IPC-Sim solves extreme nonlinear volumetric elastodynamic models using FEM. Finally, some toolboxes are developed for specific applications, such as the DiffAqua [160], an optimization toolbox for soft underwater swimming robots.

X. CONCLUSION

Providing realistic models able to be operated computationally in real time or faster, to solve direct and inverse problems of the wide variety of soft robots designed so far is an unattainable dream. Therefore, the choice of a modeling technique is the result of a compromise between realism (accuracy) and computational efficiency, which is largely dictated by the user's specific needs. For example, designers may be more interested in realism in order to capture the concept of a new actuator in a first phase, and in a second phase by computational efficiency of forward (kinematics, statics, dynamics) algorithms that can help optimization techniques requiring many simulations with different sets of design parameters. In the same way, closed-loop control strategies can allow some relaxation of accuracy in favor of designing inverse algorithms (kinematics, statics, dynamics) capable of running online. Based on this tradeoff, here follows a critical analysis of the modeling approaches presented above.

Surrogate models of Section VIII have the great advantage of being conceptually applicable to all systems, without physical modeling effort, and can provide fast dedicated algorithms compatible with real-time control. However, for each robot design, a huge database of measurements has to be built to feed the learning process.

As regards physics-based models, the only approaches that are physically consistent at all levels of modeling, (geometry, kinematics, and dynamics), are those based on continuum mechanics of Sections III–V, as well as the discrete rods method of Section VII-C. Potentially, they can be used to solve both direct problems (simulation) and inverse problems (control). Like data-driven models of Section VIII, commercial FEM software have the advantage of being applicable to complex systems of arbitrary 3-D geometry in multiphysics contexts. For these reasons, they are well suited to the design of new actuation principles or to the study of specific complex phenomena. However, they are often expensive in terms of computation time and poorly adapted to robotics specific control problems. To speed up the computations, the direct material discretizations in Sections VII-A and VII-B, may be appealing at first glance, since they allow any continuous system to be replaced by a discrete one with lumped

parameters. However, although they can provide mechanically consistent discrete formulations suited to fast simulation, they require complex identification methods to relate the lumped parameters to the distributed original ones. In this regard, it is worth mentioning that it is one of the historical motivations of the FEM to have overcame this "naive" discretization. With the same goals in mind, Sofa has made great efforts in recent years to revisit and optimize 3-D FEM for user-friendly modeling and rapid simulation of soft robots interacting with complex environments. However, due to the large number of nodal dof, all these approaches remain difficult to exploit for control purposes, and one of the challenges they face is to develop efficient reduction numerical methods compatible with the highly nonlinear character of soft robots (see Section VIII-B). When possible, a natural reduction is to consider special geometries such as shells and rods. While the former remain little represented in robotics, the latter are widely used to model multibody systems composed of rods and rigid bodies. In FEM, the use of beam-specific finite elements then becomes natural, and the GE-FEM based on Cosserat beams of Section III-B, seems to be a good choice, as it is very efficient both in terms of accuracy and computational cost. However, it still suffers from a lack of existing commercial software dedicated to robotics and is difficult to implement from scratch.

Based on the same models (based on 1-D directors), the other methods in Section IV inherently enjoy similar accuracy to that of GE-FEM, and represent reliable alternatives for soft robots that can be described as beams (or a combination of beams). This includes robots with concentric tubes, continuous parallel robots, or soft arms that do not involve large cross-sectional inflation, but also systems with thread-like actuators, such as TD-CRs. Moreover, unlike FEM, they were specifically developed for robotic purposes, whether for real-time simulation based on the shooting method, or for the design of model-based control laws. In the latter case, modal Ritz approaches as the GVS can provide highly reduced dynamic models in the usual explicit Lagrangian form of rigid robots, and thus, facilitate the transfer of methods from rigid to soft robotics. On the other hand, although computationally very efficient and ideally suited for kinematic control, the geometric approaches of Section VI-B. are based on certain kinematic simplifications that are not consistent with continuum mechanics. In particular, PCC remains mechanically consistent only for specific actuation designs and when gravity is negligible. Note that although widely used, this approach being a subcase of the fully consistent GVS, it should be advantageously replaced by this alternative approach. Regarding the other simplified models of Section VI, while functional approaches built around a reference curve, are conceptually natural and can be computationally efficient, they often struggle to capture the torsional state in a consistent way. Also note that in contrast to modeling approaches based on a direct material discretization, the discrete rod method is fully consistent since it is based from the beginning on the discrete differential geometry of the Cosserat theory (and from that point of view, should be classified into the directors based approaches of Section III-B). Moreover, it has been developed from the start for fast (interactive) simulation by the computer graphics community

and from this point of view, it represents a promising perspective for soft robotics. Finally, Table I summarizes the main modeling families in relation to their uses and robot designs.

Soft robotics was developed in the last two decades and the main efforts so far have been focuses on the simulation of the robot's static and dynamic behavior. Now the efforts of many researchers are mostly toward the extension of these approaches for control [161], [162] and for their integration with optimization tools [42], [163]. The main sources of inspiration toward the achievements of these goals are more likely to come from other research disciplines. While going through the papers of this survey, we tackled a great number of disciplines that represent their theoretical foundations: continuum and solid mechanics, computational mechanics, machine learning, computer graphics, just to name a few. This interdisciplinary is probably what makes soft robotics so interesting, attracting scientists from different research fields. On the other side, being the topic so widespread, it is not easy to grasp it and this constitutes the main motivation behind this manuscript. In this way, we were able to recognize more clearly the uniqueness and the commonalities between the different techniques that have been presented so far, in the effort to untangle such a vast research topic.

References

[1] B. Tondu and P. Lopez, "Modeling and control of Mckibben artificial muscle robot actuators," *IEEE Control Syst. Mag.*, vol. 20, no. 2, pp. 15–38, Apr. 2000.

[2] C. Laschi, B. Mazzolai, and M. Cianchetti, "Soft robotics: Technologies and systems pushing the boundaries of robot abilities," *Sci. Robot.*, vol. 1, no. 1, 2016, Art. no. eaah3690.

[3] D. Trivedi, C. D. Rahn, W. M. Kier, and I. D. Walker, "Soft robotics: Biological inspiration, state of the art, and future research," *Appl. Bionics Biomech.*, vol. 5, no. 3, pp. 99–117, 2008.

[4] D. Rus and M. T. Tolley, "Design, fabrication and control of soft robots," *Nature*, vol. 521, no. 7553, pp. 467–475, 2015.

[5] T. Thuruthel, Y. Ansari, E. Falotico, and C. Laschi, "Control strategies for soft robotic manipulators: A survey," *Soft Robot.*, vol. 5, no. 2, pp. 149–163, 2018.

[6] R. Webster and B. Jones, "Design and kinematic modeling of constant curvature continuum robots: A review," *Int. J. Robot. Res.*, vol. 29, no. 13, pp. 1661–1683, 2010.

[7] G. S. Chirikjian, "Conformational modeling of continuum structures in robotics and structural biology: A review," *Adv. Robot.*, vol. 29, no. 3, pp. 817–829, 2015.

[8] A. Chawla, C. Frazelle, and I. Walker, "A comparison of constant curvature forward kinematics for multisection continuum manipulators," in *Proc. IEEE Int. Conf. Robot. Comp.*, 2018, pp. 217–223.

[9] D. Kim et al., "Review of machine learning methods in soft robotics," *PLoS One*, vol. 16, no. 2, pp. 1–24, 2021.

[10] X. Wang, Y. Li, and K. Kwok, "A survey for machine learning-based control of continuum robots," *Front. Robot. AI*, vol. 8, 2021.

[11] J. Burgner-Kahrs, D. C. Rucker, and H. Choset, "Continuum robots for medical applications: A survey," *IEEE Trans. Robot.*, vol. 31, no. 6, pp. 1261–1280, Dec. 2015.

[12] H. B. Gilbert, "On the mathematical modeling of slender biomedical continuum robots," *Front. Robot. AI*, vol. 8, 2021.

[13] P. Rao, Q. Peyron, S. Lilge, and J. Burgner-Kahrs, "How to model tendon-driven continuum robots and benchmark modelling performance," *Front. Robot. AI*, vol. 7, 2021.

[14] F. Bullo and A. Lewis, *Geometric Control of Mechanical Systems* (Texts in Applied Mathematics 49). Berlin, Germany: Springer-Verlag, 2004.

[15] R. Murray, Z. Li, and S. Sastry, *A Mathematical Introduction to Robotic Manipulation*. Boca Raton, FL, USA: CRC Press, 1994.

[16] P. Villaggio, *Mathematical Models for Elastic Structures*. Cambridge, U.K.: Cambridge Univ. Press, 1997.

[17] R. Ogden, *Non-Linear Elastic Deformations*. New York, NY, USA: Dover Publication, 1999.

[18] F. Renda, F. Giorgio-Serchi, F. Boyer, and C. Laschi, "Modelling cephalopod-inspired pulsed-jet locomotion for underwater soft robots," *Bioinspiration Biomimetics*, vol. 10, no. 5, 2015, Art. no. 055005.

[19] F. Boyer and F. Renda, "Poincaré's equations for cosserat media: Application to shells," *J. Nonlinear Sci.*, vol. 27, pp. 1–44, 2017.

[20] F. Renda, F. Giorgio-Serchi, F. Boyer, C. Laschi, J. Dias, and L. Seneviratne, "A unified multi-soft-body dynamic model for underwater soft robots," *Int. J. Robot. Res.*, vol. 37, no. 6, pp. 648–666, 2018.

[21] E. Cosserat and F. Cosserat, *Theorie Des Corps Deformables*. Cambridge, U.K.: Cambridge Univ. Press, 1909.

[22] F. Boyer, M. Porez, and W. Khalil, "Macro-continuous computed torque algorithm for a three-dimensional EEL-like robot," *IEEE Trans. Robot.*, vol. 22, no. 4, pp. 763–775, Aug. 2006.

[23] F. Boyer, S. Ali, and M. Porez, "Macrocontinuous dynamics for hyper-redundant robots: Application to kinematic locomotion bioinspired by elongated body animals," *IEEE Trans. Robot.*, vol. 28, no. 2, pp. 303–317, Apr. 2012.

[24] F. Renda, M. Giorelli, M. Calisti, M. Cianchetti, and C. Laschi, "Dynamic model of a multibending soft robot arm driven by cables," *IEEE Trans. Robot.*, vol. 30, no. 5, pp. 1109–1122, Oct. 2014.

[25] D. B. Camarillo, C. F. Milne, C. R. Carlson, M. R. Zinn, and J. K. Salisbury, "Mechanics modeling of tendon-driven continuum manipulators," *IEEE Trans. Robot.*, vol. 24, no. 6, pp. 1262–1273, Dec. 2008.

[26] D. Rucker and R. Webster, "Statics and dynamics of continuum robots with general tendon routing and external loading," *IEEE Trans. Robot.*, vol. 27, no. 6, pp. 1033–1044, Dec. 2011.

[27] F. Renda, M. Cianchetti, H. Abidi, J. Dias, and L. Seneviratne, "Screw-based modeling of soft manipulators with tendon and fluidic actuation," *J. Mech. Robot.*, vol. 9, 2017, Art. no. 041012.

[28] F. Boyer, V. Lebastard, F. Candelier, and F. Renda, "Dynamics of continuum and soft robots: A strain parameterization based approach," *IEEE Trans. Robot.*, vol. 37, no. 3, pp. 847–863, Jun. 2021.

[29] E. Reissner, "On one-dimensional finite-strain beam theory: The plane problem," *J. Appl. Math. Phys.*, vol. 23, no. 5, pp. 795–804, 1972.

[30] A. A. Shabana, "Continuum-based geometry/analysis approach for flexible and soft robotic systems," *Soft Robot.*, vol. 5, no. 5, pp. 613–621, 2018.

[31] M. Xavier, A. Fleming, and Y. Yong, "Finite element modeling of soft fluidic actuators: Overview and recent developments," *Adv. Intell. Syst.*, vol. 3, no. 2, 2021, Art. no. 2000187.

[32] P. Moseley, J. M. Florez, H. A. Sonar, G. Agarwal, W. Curtin, and J. Paik, "Modeling, design, and development of soft pneumatic actuators with finite element method," *Adv. Eng. Mater.*, vol. 18, no. 6, pp. 978–988, 2016.

[33] C. Tawk and G. Alici, "Finite element modeling in the design process of 3D printed pneumatic soft actuators and sensors," *Robotics*, vol. 9, no. 3, 2020, Art. no. 52.

[34] J. Allard et al., "Sofa—An open source framework for medical simulation," *MMVR 15-Med. Meets Virtual Reality*, vol. 125, pp. 13–18, 2007.

[35] F. Faure et al., "Sofa: A multi-model framework for interactive physical simulation," in *Studies in Mechanobiology, Tissue Engineering and Biomaterials*. Berlin, Germany: Springer, 2012.

[36] E. Coevoet et al., "Software toolkit for modeling, simulation, and control of soft robots," *Adv. Robot.*, vol. 31, no. 22, pp. 1208–1224, 2017.

[37] G. Zheng, O. Goury, M. Thieffry, A. Kruszewski, and C. Duriez, "Controllability pre-verification of silicone soft robots based on finite-element method," in *Proc. IEEE Int. Conf. Robot. Autom.*, 2019, pp. 7395–7400.

[38] C. Duriez, "Control of elastic soft robots based on real-time finite element method," in *Proc. IEEE Int. Conf. Robot. Autom.*, 2013, pp. 3982–3987.

[39] O. Goury and C. Duriez, "Fast, generic, and reliable control and simulation of soft robots using model order reduction," *IEEE Trans. Robot.*, vol. 34, no. 6, pp. 1565–1576, Dec. 2018.

[40] O. Goury, B. Carrez, and C. Duriez, "Real-time simulation for control of soft robots with self-collisions using model order reduction for contact forces," *IEEE Robot. Autom. Lett.*, vol. 6, no. 2, pp. 3752–3759, Apr. 2021.

[41] Y. Adagolodjo, F. Renda, and C. Duriez, "Coupling numerical deformable models in global and reduced coordinates for the simulation of the direct and the inverse kinematics of soft robots," *IEEE Robot. Autom. Lett.*, vol. 6, no. 2, pp. 3910–3917, Apr. 2021.

[42] M. Bächer, E. Knoop, and C. Schumacher, "Design and control of soft robots using differentiable simulation," *Curr. Robot. Rep.*, vol. 2, no. 2, pp. 211–221, 2021.

[43] G. Maloisel, E. Knoop, C. Schumacher, and M. Bächer, "Automated routing of muscle fibers for soft robots," *IEEE Trans. Robot.*, vol. 37, no. 3, pp. 996–1008, Jun. 2021.

[44] J. Tapia, E. Knoop, M. Mutný, M. A. Otaduy, and M. Bächer, "Makesense: Automated sensor design for proprioceptive soft robots," *Soft Robot.*, vol. 7, no. 3, pp. 332–345, 2020.

[45] F. Renda, F. Boyer, J. Dias, and L. Seneviratne, "Discrete cosserat approach for multisection soft manipulator dynamics," *IEEE Trans. Robot.*, vol. 34, no. 6, pp. 1518–1533, Dec. 2018.

[46] J. Burgess, "Bending stiffness in a simulation of undersea cable deployment," *Int. J. Offshore Polar Eng.*, vol. 3, no. 3, pp. 197–204, 1993.

[47] A. A. Tjavaras, Q. Zhu, Y. Liu, M. S. Triantafyllou, and D. K. P. Yue, "The mechanics of highly-extensible cables," *J. Sound Vib.*, vol. 213, no. 4, pp. 709–737, 1998.

[48] Q. Peyron, Q. Boehler, K. Rabenorosoa, P. Renaud, and N. Andreff, "Kinematic analysis of magnetic continuum robots using continuation method and bifurcation analysis," *IEEE Robot. Autom. Lett.*, vol. 3, no. 4, pp. 3646–3653, Oct. 2018.

[49] S. Briot and A. Goldsztejn, "Singularity conditions for continuum parallel robots," *IEEE Trans. Robot.*, vol. 38, no. 1, pp. 507–525, Feb. 2021.

[50] D. Trivedi, A. Lotfi, and C. D. Rahn, "Geometrically exact models for soft robotic manipulators," *IEEE Trans. Robot.*, vol. 24, no. 4, pp. 773–780, Aug. 2008.

[51] Y. Sun, "Modelling and simulation of low-tension oceanic cable/body deployment," Ph.D. dissertation, Univ. Connecticut, Stamford, CT, USA, 1996.

[52] J. Till, V. Aloi, and D. Rucker, "Real-time dynamics of soft and continuum robots based on cosserat rod models," *Int. J. Robot. Res.*, vol. 38, no. 6, pp. 723–746, 2019.

[53] C. Gatti-Bono and N. Perkins, "Physical numerical modelling of the dynamic behavior of fly line," *J. Sound Vib.*, vol. 255, no. 3, pp. 555–577, 2002.

[54] F. Janabi-Sharifi, A. Jalali, and I. Walker, "Cosserat rod-based dynamic modeling of tendon-driven continuum robots: A tutorial," *IEEE Access*, vol. 9, pp. 68703–68719, 2021.

[55] C. B. Black, J. Till, and D. C. Rucker, "Parallel continuum robots: Modeling, analysis, and actuation-based force sensing," *IEEE Trans. Robot.*, vol. 34, no. 1, pp. 29–47, Feb. 2018.

[56] D. Rucker, R. Webster, G. Chirikjian, and N. Cowan, "Equilibrium conformations of concentric-tube continuum robots," *Int. J. Robot. Res.*, vol. 29, no. 10, pp. 1263–1280, 2010.

[57] J. Till et al., "A dynamic model for concentric tube robots," *IEEE Trans. Robot.*, vol. 36, no. 6, pp. 1704–1718, Dec. 2020.

[58] R. Featherstone, *Rigid Body Dynamics Algorithms*. New York, NY, USA: Springer2008.

[59] F. Boyer, M. Porez, A. Leroyer, and M. Visonneau, "Fast dynamics of an EEL-like robot-comparisons with Navier-Stokes simulations," *IEEE Trans. Robot.*, vol. 24, no. 6, pp. 1274–1288, Dec. 2008.

[60] F. Renda, M. Cianchetti, M. Giorelli, A. Arienti, and C. Laschi, "A 3D steady-state model of a tendon-driven continuum soft manipulator inspired by the octopus arm," *Bioinspiration Biomimetics*, vol. 7, no. 2, 2012, Art. no. 025006.

[61] A. L. Orekhov and N. Simaan, "Solving cosserat rod models via collocation and the magnus expansion," in *Proc. IEEE Int. Conf. Intell. Robots Syst.*, 2020, pp. 8653–8660.

[62] J. Simo and L. Vu-Quoc, "On the dynamics in space of rods undergoing large motions—A geometrically exact approach," *Comput. Methods Appl. Mech. Eng.*, vol. 66, no. 2, pp. 125–161, 1988.

[63] J. Simo and D. Fox, "On a stress resultant geometrically exact shell model. Part I: Formulation and optimal parametrization," *Comput. Methods Appl. Mech. Eng.*, vol. 72, no. 3, pp. 267–304, 1989.

[64] A. Cardona and M. Geradin, "A beam finite element non-linear theory with finite rotations," *Int. J. Numer. Methods Eng.*, vol. 26, no. 11, pp. 2403–2438, 1988.

[65] F. Boyer and D. Primault, "Finite element of slender beams in finite transformations: A geometrically exact approach," *Int. J. Numer. Methods. Eng.*, vol. 59, no. 5, pp. 669–702, 2004.

[66] V. Sonneville, A. Cardona, and O. Brüls, "Geometrically exact beam finite element formulated on the special euclidean group SE(3)," *Comput. Methods Appl. Mech. Eng.*, vol. 268, pp. 451–474, 2014.

[67] " LMS samtech samcef Mecano,". [Online]. Available: https://www.siemens.com/plm/lms

[68] A. Shabana, "Definition of the slopes and the finite element absolute nodal coordinate formulation," *Multibody Syst. Dyn.*, vol. 1, no. 3, pp. 339–348, 1997.

[69] C. Meier, A. Popp, and W. A. Wall, "Geometrically exact finite element formulations for slender beams: Kirchhoff–love theory versus Simo–Reissner theory," *Arch. Comput. Methods Eng.*, vol. 26, no. 1, pp. 163–243, 2019.

[70] I. Tunay, "Spatial continuum models of rods undergoing large deformation and inflation," *IEEE Trans. Robot.*, vol. 29, no. 2, pp. 297–307, Apr. 2013.

[71] S. M. H. Sadati, S. E. Naghibi, I. D. Walker, K. Althoefer, and T. Nanayakkara, "Control space reduction and real-time accurate modeling of continuum manipulators using Ritz and Ritz–Galerkin methods," *IEEE Robot. Autom. Lett.*, vol. 3, no. 1, pp. 328–335, Jan. 2018.

[72] P. Češarek, M. Saje, and D. Zupan, "Dynamics of flexible beams: Finite-element formulation based on interpolation of strain measures," *Finite Elem. Anal. Des.*, vol. 72, pp. 47–63, 2013.

[73] S. Grazioso, G. Di Gironimo, and B. Siciliano, "A geometrically exact model for soft continuum robots: The finite element deformation space formulation," *Soft Robot.*, vol. 6, no. 6, pp. 790–811, 2019.

[74] F. Renda, C. Armanini, V. Lebastard, F. Candelier, and F. Boyer, "A geometric variable-strain approach for static modeling of soft manipulators with tendon and fluidic actuation," *IEEE Robot. Autom. Lett.*, vol. 5, no. 3, pp. 4006–4013, Jul. 2020.

[75] A. T. Mathew, I. M. B. Hmida, C. Armanini, F. Boyer, and F. Renda, "SoRoSim: A MATLAB toolbox for hybrid rigid-soft robots based on the geometric variable-strain approach," *IEEE Robot. Autom. Mag.*, to be published, doi: :10.1109/MRA.2022.3202488.

[76] F. Renda, C. Messer, C. Rucker, and F. Boyer, "A sliding-rod variable-strain model for concentric tube robots," *IEEE Robot. Autom. Lett.*, vol. 6, no. 2, pp. 3451–3458, Apr. 2021.

[77] F. Boyer, V. Lebastard, F. Candelier, and F. Renda, "Extended Hamilton's principle applied to geometrically exact Kirchhoff sliding rods," *J. Sound Vib.*, vol. 516, 2022, Art. no. 116511.

[78] G. F. Carrier, "The spaghetti problem," *Amer. Math. Monthly*, vol. 56, no. 1, pp. 669–672, 1949.

[79] F. Renda and L. Seneviratne, "A geometric and unified approach for modeling soft-rigid multi-body systems with lumped and distributed degrees of freedom," in *Proc. IEEE Int. Conf. Robot. Autom.*, 2018, pp. 1567–1574.

[80] C. Armanini, I. Hussain, M. Z. Iqbal, D. Gan, D. Prattichizzo, and F. Renda, "Discrete cosserat approach for closed-chain soft robots: Application to the fin-ray finger," *IEEE Trans. Robot.*, vol. 37, no. 6, pp. 2083–2098, Dec. 2021.

[81] B. Caasenbrood, A. Pogromsky, and H. Nijmeijer, "Control-oriented models for hyperelastic soft robots through differential geometry of curves," *Soft Robot.*, 2022.

[82] C. D. Santina and D. Rus, "Control oriented modeling of soft robots: The polynomial curvature case," *IEEE Robot. Autom. Lett.*, vol. 5, no. 2, pp. 290–298, Apr. 2020.

[83] C. D. Santina, "The soft inverted pendulum with affine curvature," in *Proc. IEEE 59th Conf. Decis. Control*, 2020, pp. 4135–4142.

[84] L. U. Odhner and A. M. Dollar, "The smooth curvature model: An efficient representation of Euler–Bernoulli flexures as robot joints," *IEEE Trans. Robot.*, vol. 28, no. 4, pp. 761–772, Aug. 2012.

[85] D. Bigoni, *Nonlinear Solid Mechanics: Bifurcation Theory and Material Instability*. Cambridge, U.K.: Cambridge Univ. Press, 2012.

[86] C. Armanini, F. Dal Corso, D. Misseroni, and D. Bigoni, "From the elastica compass to the elastica catapult: An essay on the mechanics of soft robot arm," *Proc. Roy. Soc. A*, vol. 473, no. 2198, 2017, Art. no. 20160870.

[87] K. Xu and N. Simaan, "Analytic formulation for kinematics, statics and shape restoration of multi-backbone continuum robots via elliptic integrals," *ASME J. Mech. Robot.*, vol. 2, 2009, Art. no. 11006.

[88] K. Xu and N. Simaan, "Intrinsic wrench estimation and its performance index for multisegment continuum robots," *IEEE Trans. Robot.*, vol. 26, no. 3, pp. 555–561, Jun. 2010.

[89] P. Polygerinos et al., "Modeling of soft fiber-reinforced bending actuators," *IEEE Trans. Robot.*, vol. 31, no. 3, pp. 778–789, Jun. 2015.

[90] V. Cacucciolo, F. Renda, E. Poccia, C. Laschi, and M. Cianchetti, "Modelling the nonlinear response of fibre-reinforced bending fluidic actuators," *Smart Mater. Struct.*, vol. 25, no. 10, 2016, Art. no. 105020.

[91] G. Olson, R. Hatton, J. Adams, and Y. Mengüç, "An Euler–Bernoulli beam model for soft robot arms bent through self-stress and external loads," *Int. J. Solids. Struct.*, vol. 207, pp. 113–131, 2020.

[92] S. Hirose, "Biologically inspired robots: Snake-like locomotors and manipulators," *Robotica*, vol. 12, no. 3, pp. 282–282, 1994.

[93] S. Hirose and H. Yamada, "Snake-like robots," *IEEE Robot. Autom. Mag.*, vol. 16, no. 1, pp. 88–98, Mar. 2009.

[94] G. S. Chirikjian and J. W. Burdick, "A modal approach to hyper-redundant manipulator kinematics," *IEEE Trans. Robot. Autom.*, vol. 10, no. 3, pp. 343–354, Jun. 1994.

[95] G. S. Chirikjian, "Hyper-redundant manipulator dynamics: A continuum approximation," *Adv. Robot.*, vol. 9, no. 3, pp. 217–243, 1994.

[96] M. Ivanescu, M. C. Florescu, N. Popescu, and D. Popescu, "Coil function control problem for a hyperredundant robot," in *Proc. IEEE/ASME Int. Conf. Adv. Intell. Mechatron.*, 2007, pp. 1–6.

[97] I. Singh, Y. Amara, A. Melingui, P. Mani Pathak, and R. Merzouki, "Modeling of continuum manipulators using pythagorean hodograph curves," *Soft Robot.*, vol. 5, no. 4, pp. 425–442, 2018.

[98] M. Wiese, K. Rüstmann, and A. Raatz, "Kinematic modeling of a soft pneumatic actuator using cubic hermite splines," in *Proc. IEEE Int. Conf. Intell. Robots Syst.*, 2019, pp. 7176–7182.

[99] P. Rao, Q. Peyron, and J. Burgner-Kahrs, "Shape representation and modeling of tendon-driven continuum robots using Euler arc splines," *IEEE Robot. Autom. Lett.*, vol. 7, no. 3, pp. 8114–8121, Jul. 2022.

[100] K. M. Digumarti, B. Trimmer, A. T. Conn, and J. Rossiter, "Quantifying dynamic shapes in soft morphologies," *Soft Robot.*, vol. 6, no. 6, pp. 733–744, 2019.

[101] I. Gravagne, C. Rahn, and I. Walker, "Large deflection dynamics and control for planar continuum robots," *IEEE/ASME Trans. Mechatron.*, vol. 8, no. 2, pp. 299–307, Jun. 2003.

[102] B. Jones and I. Walker, "Kinematics for multisection continuum robots," *IEEE Trans. Robot.*, vol. 22, no. 1, pp. 43–55, Feb. 2006.

[103] I. Walker, "Continuous backbone "continuum" robot manipulators," *Int. Scholarly Res. Notices*, vol. 2013, 2013.

[104] C. Escande, T. Chettibi, R. Merzouki, V. Coelen, and P. M. Pathak, "Kinematic calibration of a multisection bionic manipulator," *IEEE/ASME Trans. Mechatron.*, vol. 20, no. 2, pp. 663–674, Apr. 2015.

[105] O. Lakhal, A. Melingui, and R. Merzouki, "Hybrid approach for modeling and solving of kinematics of a compact bionic handling assistant manipulator," *IEEE/ASME Trans. Mechatron.*, vol. 21, no. 3, pp. 1326–1335, Jun. 2016.

[106] T. Mahl, A. Hildebrandt, and O. Sawodny, "A variable curvature continuum kinematics for kinematic control of the bionic handling assistant," *IEEE Trans. Robot.*, vol. 30, no. 4, pp. 935–949, Aug. 2014.

[107] V. Falkenhahn, T. Mahl, A. Hildebrandt, R. Neumann, and O. Sawodny, "Dynamic modeling of bellows-actuated continuum robots using the Euler–Lagrange formalism," *IEEE Trans. Robot.*, vol. 31, no. 6, pp. 1483–1496, Dec. 2015.

[108] I. S. Godage, E. Guglielmino, D. T. Branson, G. A. Medrano-Cerda, and D. G. Caldwell, "Novel modal approach for kinematics of multisection continuum arms," in *Proc. IEEE/RSJ Int. Conf. Intell. Robots Syst.*, 2011, pp. 1093–1098.

[109] I. Godage, G. Medrano-Cerda, D. Branson, E. Guglielmino, and D. Caldwell, "Modal kinematics for multisection continuum arms," *Bioinspiration Biomimetics*, vol. 10, no. 2, 2015, Art. no. 035002.

[110] I. S. Godage, D. T. Branson, E. Guglielmino, G. A. Medrano-Cerda, and D. G. Caldwell, "Dynamics for biomimetic continuum arms: A modal approach," in *Proc. IEEE Int. Conf. Robot. Biomim.*, 2011, pp. 104–109.

[111] I. Godage, D. Branson, E. Guglielmino, G. Medrano-Cerda, and D. Caldwell, "Shape function-based kinematics and dynamics for variable length continuum robotic arms," in *Proc. IEEE Int. Conf. Robot. Autom.*, 2011, pp. 452–457.

[112] I. Godage, G. Medrano-Cerda, D. Branson, E. Guglielmino, and D. Caldwell, "Dynamics for variable length multisection continuum arms," *Int. J. Robot. Res.*, vol. 35, no. 6, pp. 695–722, 2016.

[113] R. Webster, J. Kim, N. Cowan, G. Chirikjian, and A. Okamura, "Nonholonomic modeling of needle steering," *Int. J. Robot. Res.*, vol. 25, no. 5/6, pp. 509–525, 2006.

[114] R. Webster, J. Romano, and N. Cowan, "Mechanics of precurved-tube continuum robots," *IEEE Trans. Robot.*, vol. 25, no. 1, pp. 67–78, Feb. 2009.

[115] P. Sears and P. Dupont, "A steerable needle technology using curved concentric tubes," in *Proc. IEEE Int. Conf. Intell. Robots Syst.*, 2006, pp. 2850–2856.

[116] T. F. Allen, L. Rupert, T. R. Duggan, G. Hein, and K. Albert, "Closed-form non-singular constant-curvature continuum manipulator kinematics," in *Proc. IEEE Int. Conf. Soft Robot.*, 2020, pp. 410–416.

[117] C. Della Santina, A. Bicchi, and D. Rus, "On an improved state parametrization for soft robots with piecewise constant curvature and its use in model based control," *IEEE Robot. Autom. Lett.*, vol. 5, no. 2, pp. 1001–1008, Apr. 2020.

[118] D. B. Camarillo, C. R. Carlson, and J. K. Salisbury, "Configuration tracking for continuum manipulators with coupled tendon drive," *IEEE Trans. Robot.*, vol. 25, no. 4, pp. 798–808, Aug. 2009.

[119] S. M. H. Sadati et al., "A geometry deformation model for braided continuum manipulators," *Front. Robot. AI*, vol. 4, 2017.

[120] W. Rone and P. Ben-Tzvi, "Continuum robot dynamics utilizing the principle of virtual power," *IEEE Trans. Robot.*, vol. 30, no. 1, pp. 275–287, Feb. 2014.

[121] W. S. Rone and P. Ben-Tzvi, "Mechanics modeling of multisegment rod-driven continuum robots," *J. Mech. Robot.*, vol. 6, no. 4, 2014, Art. no. 041006.

[122] P. E. Dupont, J. Lock, B. Itkowitz, and E. Butler, "Design and control of concentric-tube robots," *IEEE Trans. Robot.*, vol. 26, no. 2, pp. 209–225, Apr. 2010.

[123] R. Xu, S. F. Atashzar, and R. V. Patel, "Kinematic instability in concentric-tube robots: Modeling and analysis," in *Proc. IEEE Int. Conf. Biomed. Robot. Biomechatron.*, 2014, pp. 163–168.

[124] R. Hendrick, H. B. Gilbert, and R. J. Webster, "Designing snap-free concentric tube robots: A local bifurcation approach," in *Proc. IEEE Int. Conf. Robot. Autom.*, 2015, pp. 2256–2263.

[125] H. Habibi, C. Yang, I. S. Godage, R. Kang, I. D. Walker, and D. T. Branson, "A Lumped-Mass Model for Large Deformation Continuum Surfaces Actuated by Continuum Robotic Arms," *J. Mech. Robot.*, vol. 12, no. 1, 2019, Art. no. 011014.

[126] J. Jung, R. S. Penning, N. J. Ferrier, and M. R. Zinn, "A modeling approach for continuum robotic manipulators: Effects of nonlinear internal device friction," in *Proc. IEEE Int. Conf. Intell. Robots Syst.*, 2011, pp. 5139–5146.

[127] J. Austin, R. Corrales-Fatou, S. Wyetzner, and H. Lipson, "Titan: A parallel asynchronous library for multi-agent and soft-body robotics using Nvidia Cuda," in *Proc. IEEE Int. Conf. Robot. Autom.*, 2020, pp. 7754–7760.

[128] M. Kutzer, S. Segreti, C. Brown, M. Armand, R. H. Taylor, and S. Mears, "Design of a new cable-driven manipulator with a large open lumen: Preliminary applications in the minimally-invasive removal of osteolysis," in *Proc. IEEE Int. Conf. Robot. Autom.*, 2011, pp. 2913–2920.

[129] M. Khoshnam and R. V. Patel, "A pseudo-rigid-body 3R model for a steerable ablation catheter," in *Proc. IEEE Int. Conf. Robot. Autom.*, 2013, pp. 4427–4432.

[130] V. Venkiteswaran, J. Sikorski, and S. Misra, "Shape and contact force estimation of continuum manipulators using pseudo rigid body models," *Mech. Mach. Theory*, vol. 139, pp. 34–45, 2019.

[131] Y. Yu, L. L. Howell, C. Lusk, Y. Yue, and M. He, "Dynamic modeling of compliant mechanisms based on the pseudo-rigid-body model," *J. Mech. Des.*, vol. 127, no. 4, pp. 760–765, 2005.

[132] H. Mochiyama and T. Suzuki, "Dynamical modelling of a hyper-flexible manipulator," in *Proc. SICE Annu. Conf.*, 2002, vol. 3, pp. 1505–1510.

[133] Y. Ganji and F. Janabi-Sharifi, "Catheter kinematics for intracardiac navigation," *IEEE Trans Biomed Eng.*, vol. 56, no. 3, pp. 621–32, Mar. 2009.

[134] M. Sfakiotakis, A. Kazakidi, A. Chatzidaki, T. Evdaimon, and D. P. Tsakiris, "Multi-arm robotic swimming with octopus-inspired compliant web," in *Proc. IEEE Int. Conf. Intell. Robots Syst.*, 2014, pp. 302–308.

[135] M. Bergou, M. Wardetzky, S. Robinson, E. Audoly, and B. Grinspun, "Discrete elastic rods," *ACM Trans. Graph.*, vol. 27, no. 3, pp. 1–12, 2008.

[136] M. Bergou, B. Audoly, E. Vouga, M. Wardetzky, and E. Grinspun, "Discrete viscous threads," *ACM Trans. Graph.*, vol. 29, no. 4, pp. 1–10 2010.

[137] B. Audoly, N. Clauvelin, P.-T. Brun, M. Bergou, E. Grinspun, and M. Wardetzky, "A discrete geometric approach for simulating the dynamics of thin viscous threads," *J. Comput. Phys.*, vol. 253, pp. 18–49, 2013.

[138] M. Gazzola, L. H. Dudte, A. G. McCormick, and L. Mahadevan, "Forward and inverse problems in the mechanics of soft filaments," *R. Soc. Open Sci.*, vol. 5, no. 6, 2018, Art. no. 171628.

[139] N. Naughton, J. Sun, A. Tekinalp, T. Parthasarathy, G. Chowdhary, and M. Gazzola, "Elastica: A compliant mechanics environment for soft robotic control," *IEEE Robot. Autom. Lett.*, vol. 6, no. 2, pp. 3389–3396, Apr. 2021.

[140] N. Goldberg et al., "On planar discrete elastic rod models for the locomotion of soft robots," *Soft Robot.*, vol. 6, no. 5, pp. 595–610, 2019.

[141] W. Huang, X. Huang, C. Majidi, and M. K. Jawed, "Dynamic simulation of articulated soft robots," *Nature Commun.*, vol. 11, 2020, Art. no. 2233.

[142] V. Megaro, J. Zehnder, M. Bächer, S. Coros, M. Gross, and B. Thomaszewski, "A computational design tool for compliant mechanisms," *ACM Trans. Graph.*, vol. 36, no. 4, 2017, Art. no. 82.

[143] D. Braganza, D. M. Dawson, I. D. Walker, and N. Nath, "A neural network controller for continuum robots," *IEEE Trans. Robot.*, vol. 23, no. 6, pp. 1270–1277, Dec. 2007.

[144] A. Melingui, C. Escande, N. Benoudjit, R. Merzouki, and J. Mbede, "Qualitative approach for forward kinematic modeling of a compact bionic handling assistant trunk," *IFAC Proc. Volumes*, vol. 47, no. 3, pp. 9353–9358, 2014.

[145] A. Melingui, O. Lakhal, B. Daachi, J. B. Mbede, and R. Merzouki, "Adaptive neural network control of a compact bionic handling arm," *IEEE/ASME Trans. Mechatron.*, vol. 20, no. 6, pp. 2862–2875, Dec. 2015.

[146] M. Giorelli, F. Renda, M. Calisti, A. Arienti, G. Ferri, and C. Laschi, "Neural network and jacobian method for solving the inverse statics of a cable-driven soft arm with nonconstant curvature," *IEEE Trans. Robot.*, vol. 31, no. 4, pp. 823–834, Aug. 2015.

[147] M. Giorelli, F. Renda, M. Calisti, A. Arienti, G. Ferri, and C. Laschi, "Learning the inverse kinetics of an octopus-like manipulator in three-dimensional space," *Bioinspiration Biomimetics*, vol. 10, no. 3, 2015, Art. no. 035006.

[148] T. Thuruthel, E. Falotico, M. Manti, A. Pratesi, M. Cianchetti, and C. Laschi, "Learning closed loop kinematic controllers for continuum manipulators in unstructured environments," *Soft Robot.*, vol. 4, no. 3, pp. 285–296, 2017.

[149] T. Thuruthel, E. Falotico, F. Renda, and C. Laschi, "Learning dynamic models for open loop predictive control of soft robotic manipulators," *Bioinspiration Biomimetics*, vol. 12, no. 6, 2017, Art. no. 066003.

[150] T. G. Thuruthel, E. Falotico, F. Renda, and C. Laschi, "Model-based reinforcement learning for closed-loop dynamic control of soft robotic manipulators," *IEEE Trans. Robot.*, vol. 35, no. 1, pp. 124–134, Feb. 2019.

[151] M. Rolf and J. J. Steil, "Efficient exploratory learning of inverse kinematics on a bionic elephant trunk," *IEEE Trans. Neural. Netw. Learn. Syst.*, vol. 25, no. 6, pp. 1147–1160, Jun. 2014.

[152] D. Bruder, X. Fu, R. B. Gillespie, C. D. Remy, and R. Vasudevan, "Data-driven control of soft robots using Koopman operator theory," *IEEE Trans. Robot.*, vol. 37, no. 3, pp. 948–961, Jun. 2021.

[153] H. Arbabi and I. Mezic, "Ergodic theory, dynamic mode decomposition, and computation of spectral properties of the Koopman operator," *SIAM J. Appl. Dyn. Syst.*, vol. 16, no. 4, pp. 2096–2126, 2017.

[154] M. Thieffry, A. Kruszewski, C. Duriez, and T. Guerra, "Control design for soft robots based on reduced-order model," *IEEE Robot. Autom. Lett.*, vol. 4, no. 1, pp. 25–32, Jan. 2019.

[155] J. Chenevier, D. González, J. V. Aguado, F. Chinesta, and E. Cueto, "Reduced-order modeling of soft robots," *PLoS One*, vol. 13, no. 2, pp. 1–15, 2018.

[156] S. Sadati et al., "TMTDyn: A MATLAB package for modeling and control of hybrid rigid–continuum robots based on discretized lumped systems and reduced-order models," *Int. J. Robot. Res.*, vol. 40, no. 1, pp. 296–347, 2021.

[157] M. A. Graule, C. B. Teeple, T. P. McCarthy, G. R. Kim, R. C. St Louis, and R. J. Wood, "Somo: Fast and accurate simulations of continuum robots in complex environments," in *Proc. IEEE Int. Conf. Intell. Robots Syst.*, 2021, pp. 3934–3941.

[158] Y. Hu et al., "Chainqueen: A real-time differentiable physical simulator for soft robotics," in *Proc. IEEE Int. Conf. Robot. Autom.*, 2019, pp. 6265–6271.

[159] M. Li et al., "Incremental potential contact: Intersection-and inversion-free, large-deformation dynamics," *ACM Trans. Graph.*, vol. 39, no. 4, 2020.

[160] P. Ma et al., "Diffaqua: A differentiable computational design pipeline for soft underwater swimmers with shape interpolation," *ACM Trans. Graph.*, vol. 40, no. 4, pp. 1–14, 2021.

[161] C. Della Santina, C. Duriez, and D. Rus, "Model based control of soft robots: A survey of the state of the art and open challenges," 2021, *arXiv:2110.01358*.

[162] F. Renda, C. Armanini, A. Mathew, and F. Boyer, "Geometrically-exact inverse kinematic control of soft manipulators with general threadlike actuators' routing," *IEEE Robot. Autom. Lett.*, vol. 7, no. 3, pp. 7311–7318, Jul. 2022.

[163] C. Armanini, A. A. Alshehhi, A. T. Mathew, I. B. Hmida, C. Stefanini, and F. Renda, "Model-based design optimization of underwater flagellate propellers," *IEEE Robot. Autom. Lett.*, vol. 7, no. 4, pp. 10089–10096, Oct. 2022.

Costanza Armanini (Member, IEEE) received the B.Sc. and M.Sc. degrees in civil engineering and the Ph.D. degree in mechanical engineering from the University of Trento, Trento, Italy, in 2011, 2014, and 2018, respectively.

She is currently a Postdoctoral Fellow with the Department of Mechanical Engineering, Khalifa University, Abu Dhabi, UAE. Her research interests include continuum mechanics and structural instabilities for the development of novel technologies, with a special focus on soft robotics.

Christian Duriez (Senior Member, IEEE) received the Ph.D. degree in robotics from the University of Evry and CEA, Évry, France, in 2004.

He joined INRIA, Le Chesnay-Rocquencourt, France, in 2006 and he was promoted as the Directeur de Recherche in 2014 and is currently the Head of DEFROST Team. He is also currently the Research Director with Inria Lille–Nord Europe, Lille, France. He participated to the creation of the open-source SOFA framework. His research interests include soft robot models and control, fast finite-element methods, simulation of contact response, and new algorithms for haptics.

Frédéric Boyer received the Diploma in mechanical engineering from the Institut Nationale Polytechnique de Grenoble, Grenoble, France, in 1991, the Master of Research degree in mechanics from the University of Grenoble, Grenoble, France, in 1991, and the Ph.D. degree in robotics from the University of Paris VI, Paris, France, in 1994.

He is currently a Professor with the Department of Automatic Control, IMT-Atlantique, Nantes, France, where he is a member of the Robotics Team, Laboratoire des Sciences du Numérique de Nantes (LS2N), Nantes, France. His research interests include structural dynamics, geometric mechanics, and biorobotics.

Federico Renda (Member, IEEE) received the B.Sc. and M.Sc. degrees in biomedical engineering from the University of Pisa, Pisa, Italy, in 2007 and 2009, respectively, and the Ph.D. degree in biorobotics from the Biorobotics Institute, Scuola Superiore Sant'Anna, Pisa, in 2014.

He is currently an Associate Professor with the Department of Mechanical Engineering, Khalifa University, Abu Dhabi, UAE. His research interests include dynamic modeling and control of soft and continuum robots using principles of geometric mechanics.

Anup Teejo Mathew received the Ph.D. degree in mechanical engineering from the National University of Singapore, Singapore, in 2019.

He is currently a Postdoctoral Fellow with Khalifa University, Abu Dhabi, UAE. He has authored or coauthored several papers on topics ranging, such as soft robotics modeling, electroactive polymers, and energy harvesting. His current research interests include theoretical modeling of soft robotics and design and development of underwater soft robotics.